Evolutionary Tinkering of the Mandibular Canal Linked to Convergent Regression of Teeth in Placental Mammals

Sérgio Ferreira-Cardoso, Frédéric Delsuc, Lionel Hautier

Evolutionary tinkering of the mandibular canal linked to convergent regression of teeth in placental mammals

Sérgio Ferreira-Cardoso[1,*], Frédéric Delsuc[1,3] and Lionel Hautier[1,2,*]

Author list footnotes

[1]Institut des Sciences de l'Evolution de Montpellier (ISEM), CNRS, IRD, EPHE, Université de Montpellier, Montpellier, France.

[2]Mammal Section, Life Sciences, Vertebrate Division, The Natural History Museum, London, UK

[3]Lead contact

[*]Correspondence: sergio.ferreira-cardoso@umontpellier.fr and lionel.hautier@umontpellier.fr

SUMMARY

Loss or reduction of teeth has occurred independently in all major clades of mammals [1]. This process is associated with specialized diets, such as myrmecophagy and filter feeding [2,3], and led to an extensive rearrangement of the mandibular anatomy. The mandibular canal enables lower jaw innervation through the passage of the inferior alveolar nerve (IAN) [4,5]. In order to innervate teeth, the IAN projects ascending branches directly through tooth roots [6,5], bone trabeculae [6], or bone canaliculi (i.e. dorsal canaliculi) [7]. Here, we used micro-computed tomography (μ-CT) scans of mandibles, from eight myrmecophagous species with reduced dentition and 21 non-myrmecophages, to investigate the evolutionary fate of dental innervation structures following convergent tooth regression in mammals. Our observations provide strong evidence for a link between the presence of tooth loci and the development of dorsal canaliculi. Interestingly, toothless anteaters present dorsal canaliculi and preserve intact tooth innervation while equally toothless pangolins do not. We show that the internal mandibular morphology of anteaters has a closer resemblance to that of baleen whales [7] than to pangolins. This is despite masticatory apparatus resemblances that have made anteaters and pangolins a textbook example of convergent evolution. Our results suggest that early tooth loci innervation [8] is required for maintaining the dorsal innervation of the mandible and underlines the dorsal canaliculi sensorial role in the context of mediolateral mandibular movements. This study presents a unique example of convergent redeployment of the tooth developmental pathway to a strictly sensorial function following tooth regression in anteaters and baleen whales.

Keywords

Mandibular canal; edentulous; Convergence; Mammals; Homology.

Results

Evolution of dorsal canaliculi after tooth regression

Three-dimensional (3D) models of the mandibles, teeth, and mandibular canals of 26 species were investigated (Figure 1, S1-2). Detailed anatomical descriptions of the mandibular canal in each myrmecophagous species and sister taxa are provided as Supplemental Information (Figures S1, Data S1). A summary description of additional species used to reconstruct the ancestral condition of placental mammals is provided as Supplemental Information (Figure S2, Data S1). For cetacean comparisons, we used a dataset that was recently published by Peredo *et al.* [7]. All toothed mammals get teeth innervated and vascularized, but this innervation/vascularization only occasionally happens through dorsal canaliculi. These canaliculi correspond to narrow tubular channels that connect the mandibular canal to tooth alveoli (Figure 2*E* and *F*). The teeth of the giant otter shrew (*Potamogale velox*), the aardwolf (*Proteles cristatus*) and the dog (*Canis lupus*) are rooted in close contact with the mandibular canal, with alveoli often surrounded by trabecular bone (Figures 1, S1*I,J* and *N*). The investigated additional species revealed similar patterns with either deeply rooted teeth or trabeculae surrounding the alveoli (or both; See SI; Figure S2). These species all lack dorsal canaliculi, even for dorsally implanted teeth (e.g., aardwolf molars) (Figure S1*I*). Dorsal canaliculi were present in three (Pilosa, Cingulata and Tubulidentata) out of the 18 mammals orders sampled (including one marsupial). Ancestral reconstruction unambiguously showed that the absence of dorsal canaliculi likely represents the ancestral condition in placental mammals where alveolar branches (IAN and inferior alveolar artery, IAA**)** pass through the trabecular structure of the bone or directly through tooth roots. In contrast, armadillos (*Dasypus novemcinctus*, *D. pilosus*, and *Priodontes maximus*), sloths (*Bradypus tridactylus* and *Choloepus hoffmanni*), and the aardvark (*Orycteropus afer*), present dorsal canaliculi (Figures 1, 2*E,F*, 3*C,D*, S1, S4), the so-called "dorsal branches" as previously described in baleen whales [7], whose dorsoventral length

increases as the tooth is implanted further from the mandibular canal (Figure 2*E and F*). Most of these dorsal canaliculi are located in the anterior part of the mandible where teeth are reduced or simply missing. In the nine-banded armadillo, we observed one anterior dorsal canaliculus that divides to open in four dorsal foramina (Figures 1, S1*F*), while in the hairy long-nosed armadillo we observed a dorsal canaliculus that divides in a plexus of three branches (Figures 1, S1*G*). In the aardvark, three free dorsal canaliculi split and open in six dorsal foramina (Figures 1, S1*M*). Intraspecific variation was detected and described (Figure S4; see SI), but the presence and pattern of dorsal canaliculi is always consistent among specimens. Ontogenetic variation was studied in two species of sloths in which fetuses display dorsal canaliculi associated with vestigial teeth loci (Figure 3*A,B*). These dorsal canaliculi are still present in adults of both species despite the resorption of vestigial teeth (Figure 3*C,D*).

Surprisingly, toothless species (anteaters and pangolins) display contrasted mandibular canal morphologies (Figures 1, 2). All three investigated anteater species present dorsal canaliculi that open in small foramina (Figures 3*A*-*C*, S1*A*-*C*). These foramina are placed along the anterior flattened dorsal margin of the mandible, which defines the dental pad, with only limited intraspecific and bilateral variations among specimens of the three species (Figure S4). Ontogenetic variation is equally limited, with similar patterns of dorsal canaliculi being observed in both adults and juvenile giant anteaters (*M. tridactyla*, Figure S4*L*, *M* and *N*) and nine-banded armadillos (*D. novemcinctus*, Figure S4*A*-*F*). Conversely, pangolins lack dorsal canaliculi (Figure 3*D*), with only several minute canaliculi that are parallel to the mandibular canal, both dorsally and ventrally, but rarely connected to it (Figure 1). Foramina associated to these parallel canaliculi are scarce, invisible to the naked eye, and only occasionally open dorsally to the mandibular canal.

Histological evidence for the passage of nerves and blood vessels in dorsal canaliculi

Three-dimensional analyses were complemented by histological series, which enabled to identify internal soft structures associated to the dorsal canaliculi. The LFB (see Method details in STAR methods) stained histological slices of the collared anteater (*T. tetradactyla*) mandible enabled us to describe the soft tissues encapsulated in the mandibular canal (Figure 4). We observed dorsal canaliculi that allow for the passage of an ascending branch of the inferior alveolar nerve (IANab; Figure 4*C,C*'), of the inferior alveolar artery (IAAab; Figure 4*C*), and of the inferior alveolar vein (IAVab; Figure 4*B*'). In *T. tetradactyla*, a keratinous dental pad (pa) covers the dorsal part of the mandible (Figure 4*C*). Ventrally, the epidermis (ep) consists of a small layer (Figure 4*C*), which lies dorsally to a thick dermis layer (de; Figure 4*C*). In addition to connective tissue, this dermis layer presents small blood vessels and nerve branches. Histological slices of bowhead whale [9] (Figure S3) show a similar structuration of soft tissues, with accessory branches and large IAN and IAA that most likely connect the mandibular canal to the vestigial tooth alveoli through dorsal canaliculi. The histological section [9] suggests a pronounced anterior projection of the dorsal canaliculi, similar to the pattern for the IAN ascending branches in odontocetes [4].

Discussion

Shadows of regressed tooth buds in dorsal canaliculi

Enamelless sloths, armadillos, and aardvarks all present dorsal canaliculi that are associated with either tooth alveoli or vestigial tooth loci in the anterior part of the mandible. The corresponding nervous and vascular ascending branches should then be considered homologous to alveolar branches. If the number and shape of alveolar branches can vary [6,10], especially in terminal bifurcations, each main alveolar branch usually corresponds to a single tooth root [6]. Establishing the direct homology between ascending and alveolar branches in anteaters is hindered by the absence of teeth. However, their closest relatives, sloths and armadillos, as well as the aardvark, also display some anterior dorsal canaliculi with no apparent

connection to tooth alveoli (Figures 1, 2, S1, S2). Long-nosed armadillos present dorsal canaliculi in the anterior part of the mandible and the anterior most alveoli, while sloths present minute dorsal canaliculi in cheek teeth. This suggests that dorsal canaliculi likely evolved concomitantly with tooth simplification in cingulatans and pilosans. All these species have been shown to display vestigial tooth buds in the anterior part of the mandible during pre-natal development [11–13]. The observed pattern of anterior dorsal canaliculi in long-nosed armadillos (*Dasypus*) and the aardvark roughly matches the distribution of previously described vestigial teeth [12,14–16]. In nine-banded armadillos, we found dorsal canaliculi that consistently split into three to six distinct dorsal foramina in the anterior part of the mandibles (Figure 1, S1*F*,S4*A*-*F*), while Martin [12] identified five to six vestigial incisors. This difference is not surprising given the frequent dental formula variation observed in nine-banded armadillos [17]. The observed variation in dorsal canaliculi count of anteaters and nine-banded armadillos (Figures 1, S4) was to be expected as the number and shape of alveolar branches vary in humans [6,10], both at the intraspecific and bilateral levels. This variation also matches the variation observed in tooth count of placentals showing a reduced dentition such as the aardvark [13], long-nosed armadillos [17] and the giant armadillo [18]. Such bilateral variation in tooth number might result from the lack of stabilizing selection due to an absence of strict occlusion, as hypothesized for mysticetes [9]. In the aardvark [15], the lower milk dentition is normally composed of eight to ten teeth, with the second generation of teeth varying from five to eight in number depending on the presence of vestigial anterior premolars and canines [15,16]. We found dorsal canaliculi that could correspond to two-four anterior premolars, one canine and three incisors (Figure S1*M*). This number coincides with the deciduous dental formula of the aardvark [13]. Our observations therefore provide convincing evidence for a link between the presence of teeth, vestigial or not, and the development of dorsal canaliculi.

This developmental link was corroborated by the study of ontogenetic series of both extant sloth genera. Comparisons between sloth pre- and post-natal stages allowed us to directly

145 associate one long anterior dorsal canaliculus to a vestigial tooth locus (Figure 3), which is
146 resorbed during development and is absent in adults. Based on histological sections (Figure 4),
147 we showed that ascending branches of the IAN and IAA pass through dorsal canaliculi in the
148 collared anteater (*T. tetradactyla*). Teeth innervation was likely retained after tooth resorption in
149 all pilosans, and this could extend to all xenarthrans if we consider the anterior dorsal canaliculi
150 of armadillos as representative of vestigial tooth loci. Wadu *et al.* [6] showed that human tooth
151 nerve bundles can also be retained – although slightly reduced – after tooth loss induced by
152 senescence. Our observations of histological sections of toothless whale fetuses (see [9] and SI,
153 Figure S3) suggest that vestigial tooth loci are associated to IAN and IAA ascending branches
154 during development, a situation that mirrors the condition observed in toothed cetaceans [4,5].
155 Ridgway et al. [4] described an elongation of the ascending branches of the inferior alveolar
156 nerve in dolphins, while an anterodorsal inclination was also reported for the dorsal canaliculi of
157 mysticetes [7]. However, the homology between alveolar branches and ascending branches
158 carried by dorsal canaliculi was recently challenged for whales [7]. Instead, Peredo *et al.* [7]
159 proposed that dorsal canaliculi and associated foramina constitute a derived character of crown
160 Mysticeti since no internal evidence of such a structure was visible in other edentulous taxa [7].
161 Our results clearly contradict this assertion, as we showed that anteaters display both foramina
162 and dorsal canaliculi. In our view, the ascending branches of IAN and IAA should be considered
163 as homologous to alveolar branches since they include identical structures and are linked to the
164 development of teeth. This implies that dorsal canaliculi evolved convergently in xenarthrans,
165 aardvarks, and baleen whales following tooth reduction.

166 Unlike the other toothless species investigated, pangolins do not present dorsal canaliculi in
167 their mandibles. The small parallel canaliculi (Figure S1*D*,*E*) present a distinct shape and
168 topology hindering a hypothetical homology with the dorsal canaliculi. Tims [19] reported the
169 presence of 13 to 14 tooth rudiments in the mandible of *M. javanica*, which he also compared to
170 hair follicles. However, the observed number of up to four tooth vestiges per coronal slice [19]

seems inconsistent with the position of the teeth along an anteroposterior axis. Unless *M. javanica* presents four tooth generations, no more than two tooth buds should be expected for each coronal slice [9,20]. In this context, the 13-14 teeth reported by Tims (1908) should be considered with caution and might correspond to distinct structures. The lack of tooth buds [21] might therefore explain the absence of dorsal canaliculi. Although an early dental lamina may be present in pangolin embryos [14,19], its development appears to be drastically reduced when compared to anteaters [21]. On the other hand, the lack of these structures in pangolins could be explained by phylogenetic constraints. Since dorsal canaliculi are also absent in carnivorans (Figures 1, S1*I,J*), their absence might represent the ancestral state for Ferae (Pholidota + Carnivora). Additionally, complete tooth loss probably happened much earlier in pangolins than in anteaters, since the almost certainly toothed most recent common ancestor (MRCA) of Pilosa (~58 Mya, [22]) is much more recent than the MRCA of Ferae (~80 Mya; [23]). With the oldest fossil pangolin (~45 Mya,[24]) being already toothless, the absence of dorsal canaliculi in pangolins might simply reflect a more ancient tooth loss. Importantly, our study shows that the external resemblances of the mandibles in anteaters and pangolins, which made them a textbook example of convergent evolution, have overshadowed the complex evolution of their internal morphology.

Functional role of dorsal canaliculi in toothless species

Previous studies proposed that mammalian teeth might play a sensorial role in detecting a wide array of external stimuli including pressure, proprioception, and percussion [25] in addition to their role for food intake. Our results suggest that the development of dorsal canaliculi might be linked to the presence of tooth loci/vestigial teeth in both anteaters and baleen whales. One puzzling fact however is that the development of vestigial teeth remained preserved for so long during the evolutionary history of these taxa. In sloths, Hautier *et al.* [11] showed that the mineralization and resorption of the vestigial teeth is an integral part of prenatal dental

development. Given the conservatism of sloth dental formula in the fossil record [26], they proposed that these vestiges were kept for at least 30 million years [22,26], which implies that there is still a strong selective pressure for developing these structures. Such a complex and energetically costly developmental pathway might be the consequence of a strong developmental constraint in preserving the associated innervation and vascularization of the mandible. A similar developmental constraint was proposed for the initial development of a normal eye in blind cavefish [27]. These fish present normal eye development before showing sign of later degeneration. Given that there is no separation between cells giving rise to the retina and to the forebrain at the early stage of the nervous system (neural plate stage), the development of a viable embryo with a well-formed forebrain implies the early development of the eyes [27]. Tooth innervation develops synchronously with tooth development, being controlled by local molecular signals [8]. We therefore argue that tooth development, even in initiation stages, might be required for maintaining the dorsal innervation of the mandible. As a matter of fact, embryos of pygmy anteaters present early tooth development (dental lamina-tooth buds) [21,28].

Histological slices allowed revealing the presence of dorsal projections of the IAN and IAA passing through the dorsal canaliculi in a mandible of the collared anteater. We propose that these structures respectively innervate and vascularize the mandibular keratinous pad that covers most of the dorsal margin of the horizontal ramus (Figure 4*C*). The oral sensory receptors that project via the IAN (a branch of the trigeminal nerve) may confer a somatosensory role to the mandibular keratinous pad. In fact, the pattern of innervation of this keratinous pad resembles that of bird beak [29]. Both structures display a superficial keratinous layer followed dorsally by epidermis and a large dermis with blood vessels and free nerve endings [29] (Figure 4). Early tooth development (bud stage) was previously reported in anteaters [21]. In birds, the keratinous ramphoteca was proposed to be responsible for the early interruption of odontogenesis at the lamina stage [30]. An early keratinization might be the triggering event for

subsequent odontogenesis disruption during the development of both anteater keratinous pad and bird beak. Interestingly, toothless whales also present keratinous structures (baleens) that develop after odontogenesis interruption [9]. Thewissen *et al*. [9] argued that tooth development is a *sine qua non* condition to the development of baleens. This is in line with both fossil and molecular evidence suggesting a step-wise transition between teeth and baleen in mysticetes [3]. Ekdale et al. [31] also recently suggested that foramina for baleen vascularization in the upper jaw of toothless whales are likely homologous to tooth alveoli. Similarly, odontogenesis and associated dorsal canaliculi might be a prerequisite for mandibular keratinization in anteaters. Accordingly, the lack of keratinous pad and vestigial teeth might explain the absence of dorsal canaliculi in pangolins.

In rorqual whales, the peculiar distribution of dorsal canaliculi along the mandible was proposed to be related to movement coordination of lower jaws and alignment with the baleen plates during filter feeding [7]. Pyenson *et al.* [32] argued that nerves passing through the most anterior canaliculus connected the brain to a symphyseal organ/vibrissae system responsible for mandibular motor coordination and prey detection, respectively. Given the absence of external vibrissae in anteaters and the fact that they mainly use olfaction to detect their prey [33], dorsal canaliculi and respective extensions of the IAN are unlikely related to prey detection. However, several studies [34 and references therein] described the synchronization between tongue protrusion and mandible closing during feeding in anteaters (i.e. *Myrmecophaga* and *Tamandua*) as well as in ant-eating echidnas. In these groups, the mandibles rotate medio-laterally, with the oral cavity widening when the tongue is retracted and narrowing when it is protruded, forming a tube-like mouth to serve as physical support [34,35]. This type of integrated movement would require a tactile feedback originating from the dorsal margin of the mandible, which is in contact with the protruding tongue and the upper jaw. A similar hypothesis has been proposed in whales [7] for the coordination between mandibles and baleens during gulping. Tooth pulp stimulation was shown to trigger a response of the digastric muscle in cats [36]. Dong *et al.* [37] also

showed that cat teeth stimulation results in discharge signatures for different textures (e.g., rough or smooth). Furthermore, teeth are known to respond to non-painful stimuli in humans [38]. We propose that the ascending branches of the IAN might be part of the somatosensory system involved in mechanoreception, which could explain the convergent evolution of dorsal canaliculi in the toothless mandibles of baleen whales and anteaters. In contrast, no medio-lateral rotation of the mandibles was reported in pangolins [35], while the presence of a fused symphysis likely helps maintaining the tube-like shape of the oral cavity while feeding [39]. Compared to anteaters and baleen whales, such a relatively reduced mandibular mobility could potentially explain the absence of dorsal canaliculi in pangolins.

Our results support the hypothesis of convergent exaptation of the dorsal canaliculi in anteaters and baleen whales following tooth regression. We unequivocally showed that the IAN as well as blood vessels branch through the dorsal canaliculi, and argue that keratinous structures and vestigial teeth have a crucial role in mandibular innervation, maintaining the sensorial function associated to the presence of teeth while strong selective pressures induced their loss. Despite the superficial resemblance of the masticatory apparatus between anteaters and pangolins, convergent tooth loss resulted in divergent structures in the internal morphology of their mandible. We propose that these differences likely reflect divergent phylogenetic histories and/or divergent functional constraints. Rewiring of the mandibular canal in anteaters and baleen whales provides a striking example of evolutionary tinkering linked to the regression of teeth.

Acknowledgements

We thank Steffen Bock, Peter Giere, Frieder Mayer, and Detlef Willborn (MfN), Roberto Portela Miguez, Louise Tomsett, Farah Ahmed, Amin Garbout, and Brett Clark (BMNH), Renaud

Lebrun, François Catzeflis, Pierre-Henri Fabre, and Quentin Martinez (ISEM), Guillaume Billet (MNHN), and Chris Conroy (MVZ) for access to collections and assistance with µ-CT scanning. We also thank Pierre-Henri Fabre, Chris Emerling, and two anonymous reviewers for helpful comments on the manuscript, and Quentin Martinez, Mélanie Debiais-Thibaud, and Helder Gomes Rodrigues for fruitful discussions. We acknowledge J.G.M. Thewissen and the North Slope Borough Department of Wildlife Management for Figure S3*A*. We thank Nelly Pirot, Florence Bernex, and Marion Olive (INSERM) for assistance with histology. Finally, we thank Sarah Jones who helped to improve the English of the manuscript. S.F.-C., L.H. and F.D. were supported by a European Research Council (ERC) consolidator grant [ConvergeAnt #683257]. S.F.C. benefitted from the SYNTHESYS Project (Project 312253) founded by the European Community Research Infrastructure Action under the FP7 Integrating Activities Programme. L.H. and F.D. were supported by Centre National de la Recherche Scientifique (CNRS). This work has been supported by “Investissements d’Avenir” grants managed by Agence Nationale de la Recherche Labex CEBA (ANR-10-LABX-25-01), Labex CEMEB (ANR-10-LABX-0004), and Labex NUMEV (ANR-10-LABX-0020). This is contribution ISEM 2018-275 of the Institut des Sciences de l’Evolution de Montpellier.

Author contributions

S.F.-C., L.H., F.D. collected the data, conceived the study, designed the study. S.F.-C., L.H., F.D. contributed to discussion, drafted and edited the manuscript. L.H., F.D. coordinated the study. All authors gave final approval for publication.

Declaration of Interests

The authors declare no competing interest.

References

1. Meredith, R.W., Gatesy, J., Murphy, W.J., Ryder, O.A., and Springer, M.S. (2009). Molecular decay of the tooth gene enamelin (ENAM) mirrors the loss of enamel in the fossil record of placental mammals. PLoS Genet. *5*, e1000634.

2. Meredith, R.W., Gatesy, J., and Springer, M.S. (2013). Molecular decay of enamel matrix protein genes in turtles and other edentulous amniotes. BMC Evol. Biol. *13*, 20.

3. Deméré, T.A., McGowen, M.R., Berta, A., and Gatesy, J. (2008). Morphological and molecular evidence for a stepwise evolutionary transition from teeth to baleen in mysticete whales. Syst. Biol. *57*, 15–37.

4. Ridgway, S.H., Green, R.F., and Sweeney, J.C. (1975). Mandibular anesthesia and tooth extraction. J. Wildl. Deseases *11*, 415–418.

5. Gray, H. (1995). Anatomy, descriptive and surgical (Bristol: Parragon Book Service Ltd.).

6. Wadu, S.G., Penhall, B., and Townsend, G.C. (1997). Morphological variability of the human inferior alveolar nerve. Clin. Anat. *10*, 82–87.

7. Peredo, C., Pyenson, N., Uhen, M., and Marshall, C. (2017). Alveoli, teeth, and tooth loss: understanding the homology of internal mandibular structures in mysticete cetaceans. PLoS One *12*.

8. Fried, K., Lillesaar, C., Sime, W., Kaukua, K., and Patarroyo, M. (2007). Target finding of pain nerve fibers: neural growth mechanisms in the tooth pulp. Physiol. Behav. *92*, 40–45.

9. Thewissen, J.G.M., Hieronymus, T.L., George, J.C., Suydam, R., Stimmelmayr, R., and McBurney, D. (2017). Evolutionary aspects of the development of teeth and baleen in the bowhead whale. J. Anat. *230*, 549–566.

10. Kieser, J., Kieser, D., and Hauman, T. (2005). The course and distribution of the inferior alveolar nerve in the edentulous mandible. J. Craniofac. Surg. *16*, 6–9.

11. Hautier, L., Gomes Rodrigues, H., Billet, G., and Asher, R.J. (2016). The hidden teeth of sloths: evolutionary vestiges and the development of a simplified dentition. Sci. Rep. *6*, 27763.

12. Martin, B. (1916). Tooth development in *Dasypus novemcinctus*. J. Morphol. *27*, 647–961.

13. Anthony, R. (1934). La dentition de l'oryctérope. Morphologie, développement, structure, interprétation. Ann. Sci. Nat. Zool. *17*, 289–322.

14. Spurgin, A.M. (1904). Enamel in the teeth of an embryo edentate (*Dasypus novemcinctus* linn). Am. J. Anat. *3*, 75–84.

15. Thomas, O. (1889). A milk dentition in Orcyteropus. Proc. R. Soc. London *47*, 246–248.

16. Lönnberg, E. (1906). On a new Orycteropus from Northern Congo and some remarks on the dentition of the Tubulidentata. Ark. för Zool. *3*, 31–66.

17. Ciancio, M.R., Castro, M.C., Galliari, F.C., Carlini, A.A., and Asher, R.J. (2012). Evolutionary implications of dental eruption in *Dasypus* (Xenarthra). J. Mamm. Evol. *19*, 1–8.

18. Vizcaíno, S.F., Paleobiology, S., Summer, N., and Vizcaino, S.F. (2009). Paleontological Society The Teeth of the " Toothless ": Novelties and Key Innovations in the Evolution of Xenarthrans. *35*, 343–366.

19. Tims, H.W. (1908). Tooth-vestiges and associated mouth parts in the Manidae. J. Anat. Physiol. *42*, 375–87.

20. Ishikawa, H., and Amasaki, H. (1995). Development and physiological degradation of tooth buds and development of rudiment of baleen plate in southern minke whale, Balaenoptera acutorostrata. J. Vet. Med. Sci. *57*, 665–670.

21. Rose, C. (1892). Beitrage zur Zahnentwicklung der Edentaten. Anat. Anz. *7*, 495–512.

22. Gibb, G., Condamine, F., Kuch, M., and Enk, J. (2016). Shotgun mitogenomics mrovides a reference phylogenetic framework and timescale for living xenarthrans. Mol. Biol. Evol. *33*, 621–642.

23. Meredith, R., Janečka, J., Gatesy, J., Ryder, O., Fisher, C.F., Teeling, E.C., Goodbla, A., Eizirik, E., Simão, T.L.L., and Stadler, T. (2011). Impacts of the Cretaceous terrestrial revolution and KPg extinction on mammal diversification. Science (80-.). *334*, 521–24.

24. Gaudin, T.J., Emry, R.J., and Wible, J.R. (2009). The phylogeny of living and extinct pangolins (Mammalia, Pholidota) and associated taxa: a morphology based analysis. J. Mamm. Evol. *16*, 235–305.

25. Nweeia, M.T., Eichmiller, F.C., Hauschka, P. V., Donahue, G.A., Orr, J.R., Ferguson, S.H., Watt, C.A., Mead, J.G., Potter, C.W., Dietz, R., *et al.* (2014). Sensory ability in the narwhal tooth organ system. Anat. Rec. *297*, 599–617.

26. Gaudin, T.J. (2004). Phylogenetic relationships among sloths (Mammalia, Xenarthra, Tardigrada): the craniodental evidence. Zool. J. Linn. Soc. *140*, 255–305.

27. Rétaux, S., and Casane, D. (2013). Evolution of eye development in the darkness of caves: adaptation, drift, or both? Evodevo *4*.

28. Gervais, P. (1867). Zoologie et paléontologie générales: nouvelles recherches sur les animaux vertébrés vivants et fossiles A. Bertrand, ed. (Paris: La Societé de Géographie).

29. Kuenzel, W.J. (2007). Neurobiological basis of sensory perception: welfare implications of beak trimming. Poult. Sci. *86*, 1273–82.

30. Louchart, A., and Viriot, L. (2011). From snout to beak: The loss of teeth in birds. Trends Ecol. Evol. *26*, 663–673.

31. Ekdale, E.G., Deméré, T.A., and Berta, A. (2015). Vascularization of the Gray Whale Palate (Cetacea, Mysticeti, *Eschrichtius robustus*): Soft Tissue Evidence for an Alveolar Source of Blood to Baleen. Anat. Rec. *298*, 691–702.

32. Pyenson, N., Goldbogen, J., Vogl, A., and Szathmary, G. (2012). Discovery of a sensory organ that coordinates lunge feeding in rorqual whales. Nature *485*, 498–501.

33. Lubin, Y., and Montgomery, G. (1981). Defenses of *Nasutitermes* termites (Isoptera, Termitidae) against *Tamandua* anteaters (Edentata, Myrmecophagidae). Biotropica *13*, 66–76.

34. Naples, V. (1999). Morphology, evolution and function of feeding in the giant anteater (Myrmecophaga tridactyla). J. Zool. *249*, 19–41.

35. Endo, H., Ito, K., Watabe, H., Nguyen, S., and Koyabu, D. (2017). Macroscopic and CT examinations of the mastication mechanism in the southern tamandua. Mammal Study *42*, 89–96.

36. Boissonade, F.M., and Matthews, B. (1993). Responses of trigeminal brain stem neurons and the digastric muscle to tooth-pulp stimulation in awake cats. J. Neurophysiol. *69*, 174–186.

37. Dong, W.K., Chudler, E.H., and Martin, R.F. (1985). Physiological properties of intradental mechanoreceptors. Brain Res., 389–395.

38. Chatrian, G.E., de Lima, V.M.F., Lettich, E., Canfield, R.C., Miller, R.C., and Soso, M.J. (1982). Electrical stimulation of tooth pulp in humans. II. Qualities of sensations. Pain *14*, 233–246.

39. Endo, H., Nishiumi, I., Kurohmaru, M., Nabhitabhata, J., Chan-Ard, T., Nadee, N., Agungpriyono, S., and Yamada, J. (1998). The functional anatomy of the masticatory muscles of the Malayan pangolin, Manis javanica. Mammal Study *23*, 1–8.

40. Kumar, S., Stecher, G., Suleski, M., and Hedges, S.B. (2017). TimeTree: a resource for timelines, timetrees, and divergence times. Mol. Biol. Evol. *34*, 1812–19.

Figure legends

Figure 1. Evolution of dorsal canaliculi linked to tooth regression in 28 placentals and 1

marsupial. Circular timetree (according to Kumar *et al.* [40]) with corresponding 3D reconstructions of the internal mandibular morphology with dorsal canaliculi (orange), mandibular canal (cyan), mental branches (pink), and teeth (dark blue). Tree branches are colored in orange (presence of dorsal canaliculi) and black (absence of dorsal canaliculi). Animal silhouettes are colored in black (sampled species) and gray (species from [7]).

Figure 2. Evolution of dorsal canaliculi after tooth regression. (A) *Cyclopes didactylus*; (B) *Tamandua tetradactyla*; (C) *Myrmecophaga tridactyla*; (D) *Manis javanica*; (E) *Orycteropus afer*; (F) *Priodontes maximus*. Bone is transparent. Dorsal canaliculi – orange; mental branches – purple; mandibular canal – cyan; teeth – dark blue. Scale in mm.

Figure. 3. Ontogenetic evidence of the association of dorsal canaliculi to vestigial tooth alveoli. 3D models of the mandibles of sloth fetuses (A) *Bradypus tridactylus* and (B) *Choloepus didactylus*) and adults (C) *B. tridactylus* and (D) *Choloepus hoffmanni* in medial (A, C and D) and lateral (B) views. Bone is transparent. B is a mirrored lateral view for a better perspective of the dorsal canaliculus. Dorsal canaliculi – orange; mental branches – purple; mandibular canal – cyan; teeth – dark blue. Zoomed details of the dorsal canaliculi associated with the vestigial teeth are shown. Scale in mm.

Figure 4. Histological evidence for the passage of blood vessels and nerves in dorsal canaliculi. (A) 3D-model of a mandible with a purple dashed rectangle indicating where the sagittal cut was performed; black dashed rectangles indicate the limits of the coronal cut. (B) Coronal cut showing the mandibular canal and a dorsal canaliculus; soft tissues are present dorsally to the mandibular canal, the dorsal canaliculus and the external dorsal, and dorso-

lateral surfaces of the mandible; the red square represents the area of interest to be zoomed in (B'); the purple dashed line represents the sagittal section performed on the cut portion of the mandible (A). (C) Sagittal section showing the mandibular canal, two dorsal canaliculi and associated soft tissues; soft tissues on the dorsal surface of the mandible are identified; the red square delimits the area zoomed in (C'). (C') An ascending branch of the IAN is present in the dorsal canaliculus. Abbreviations: *bo* bone; *de* dermis; *ep* epidermis; *IAA* inferior alveolar artery; *IAAab* inferior alveolar artery ascending branch; *IAN* inferior alveolar nerve; *IANa* inferior alveolar nerve accessory branch; *IANab* inferior alveolar nerve ascending branch; *IAV* inferior alveolar vein; *IAVab* inferior alveolar vein ascending branch; *pa* keratinous dentary pad.

Supplemental figure legends

Figure S1. 3D models of fourteen mandibles (five toothless and nine toothed) in lateral view. Related to Figure 1. (A) *Cyclopes didactylus* (MNHN 1986-1115); (B) *Tamandua tetradactyla* (BMNH 34.9.2.196); (C) *Myrmecophaga tridactyla* (ISEM – 065 V); (D) *Manis crassicaudata* (BMNH_67.4.12.298); (E) *Manis javanica* (BMNH 9.1.5.858); (F) *Dasypus novemcinctus* (USNM 033867); (G) *Dasypus pilosus* (ZMB 19240); (H) *Priodontes maximus* (ZMB 47528); (I) *Proteles cristatus* (BMNH 34.11.1.5); (J) *Canis lupus* (LAMC 23010); (K) *Bradypus tridactylus* (MNHN 1999-1065); (L) *Choloepus hoffmanni* (Hautier pers. Coll.); (M) *Orycteropus afer* (BMNH 27.2.11.113); (N) *Potamogale velox* (ZMB 71587). Bone is transparent. Dorsal canaliculi (numbered) – orange; mental branches (mb) – purple; mandibular canal – cyan; parallel canaliculi – yellow. Scale in mm.

Figure S2. 3D models of 12 toothed mandibles in lateral view. Related to Figure 1. (A) *Dasyurus hallucatus* (TMM M-6921); (B) *Lemur catta* (DPC-O92); (C) *Cynocephalus volans*

(FMNH 56521); (D) *Procavia capensis* (UMZC H4980K); (E) *Tapirus indicus* (KUPRI 506); (F) *Tenrec ecaudatus* (Martinez pers. coll.); (G) *Lepus europaeus* (DMET-RN1); (H) *Talpa europaea* (Martinez pers. coll.); (I) *Tupaia montana* (FMNH 108831); (H) *Rhynchocyon petersi* (BMNH 55149); (K) *Rattus norvegicus* (HACB-RN1); (L) *Molossus molossus* (AMNH 234923). Bone is transparent. Mental branches (mb) – purple; mandibular canal – cyan; teeth – dark blue; trabeculae – green. Scale in mm.

Figure S3. Histological slice of coronal sections of the mandibles of a bowhead whale and a collared anteater. Related to Figure 4. Coronal sections of the mandibles of (A) *Balaena mysticetus* [9] and (B) a formalin preserved *Tamandua tetradactyla* (ISEM 778N; LFB stained). For B bone tissue is colored in dark blue and soft tissues stained in different tones of blue and purple. The dark blue colored myelin layers can be observed. Coronal cuts showing the mandibular canal and dorsal canaliculi; soft tissues are present on mandibular canals and dorsal canaliculi. *bo* bone; *IAA* inferior alveolar artery; *IAAa* inferior alveolar artery accessory branch; *IAAab* inferior alveolar artery ascending branch; *IAN* inferior alveolar nerve; *IANa* inferior alveolar nerve accessory branch; *IANab* inferior alveolar nerve ascending branch; *IAV* inferior alveolar vein; *IAVab* inferior alveolar vein ascending branch; *vt* vestigial tooth (1st generation).

Figure S4. 3D models showing intraspecific variation of dorsal canaliculi. Related to Figures 1 and 2. (A-F) *Dasypus novemcinctus* (USNM 033867, BMNH 11.10.27.3, LSUMZ 8538, LSUMZ 29160, ZMB 84-357, USNM 020920); (G-H) *Cyclopes didactylus* (MNHN 1986-1115, BMNH 24.12.4.68); (I-K) *Tamandua tetradactyla* (BMNH 34.9.2.196, MVZ 153482, ISEM 778N); (L-N) *Myrmecophaga tridactyla* (ISEM 065V, MVZ 185238, ISEM 071N). Teeth are segmented in (A) only. Bone is transparent. Dorsal canaliculi – orange; mental branches – purple; mandibular canal – cyan; teeth – dark blue. Scale in mm.

Figure S5. Ancestral state reconstruction of the presence/absence of dorsal canaliculi in

28 placental and one marsupial species. Related to Figure 1. Posterior probabilities (%) for the presence of dorsal canaliculi are presented for each node. Presence of dorsal canaliculi – orange; absence of dorsal canaliculi – cyan.

STAR * methods

- Key resources table
- Contact for resource sharing
- Method details
- Data and software availability

Contact for resource sharing

Further information and requests for resources should be directed to, and will be fulfilled by the Lead author Frédéric Delsuc (frederic.delsuc@umontpellier.fr).

Method details

Comparative anatomy

We present an anatomical description of the mandibles and mandibular canals of 26 species (Figure 1) representing the following taxa: Vermilingua (anteaters) – *Cyclopes didactylus*, *Tamandua tetradactyla*, *Myrmecophaga tridactyla* (juvenile + adult); Cingulata (armadillos) – *Dasypus novemcinctus*, *Dasypus pilosus*, *Priodontes maximus*; Folivora (sloths) – *Bradypus tridactylus* (fetus + adult); *Choloepus* spp. (fetus + adult); Tubulidentata (aardvarks) – *Orycteropus afer*; Afrosoricida (tenrecs) – *Potamogale velox*, *Tenrec ecaudatus*; Macroscelidea (elephant shrews) – *Rhynchocyon petersi*; Hyracoidea (hyraxes) – *Procavia capensis*; Pholidota (pangolins) – *Manis crassicaudata*, *Manis javanica*; Carnivora (carnivores) – *Proteles cristatus* and *Canis lupus*; Perissodactyla (odd-toed ungulates) – *Tapirus indicus*; Chiroptera (bats) – *Molossus molossus*; Eulipotyphla (moles and shrews) – *Talpa europaea*; Lagomorpha (hares and rabbits) – *Lepus europaeus*; Rodentia (rodents) – *Rattus norvegicus*; Primates (primates) – *Lemur catta*; Dermoptera (colugos) – *Cynocephalus volans*; Scandentia (tree shrews) – *Tupaia montana*; *Dasyuromorphia* (carnivorous marsupials) – *Dasyurus hallucatus*. Using this dataset, we were able to compare the morphology of the mandibular canal and dorsal canaliculi of closely related toothed and toothless taxa, as well as a wide range of species belonging to 18 mammalian orders. We additionally compared our results to the previously published research on cetaceans and even-toed ungulates (Cetartiodactyla) by Peredo *et al.* [7]. We segmented a total of five *D. novemcinctus*, three *M. tridactyla* (two adults + one juvenile), three *T. tetradactyla*, and two *Cy. didactylus* in order to account for intraspecific variation. We also segmented left and right hemi-mandibles of the anteater specimens to assess the level of bilateral variation in dorsal canaliculi count. Both fetus and adult specimens of *B. tridactylus* and *Choloepus* spp. were studied (Figure 3) in order to seek the presence of a dorsal canaliculus linked to the development of vestigial teeth [11] and to confirm that there was no major variation in the number of dorsal canaliculi through ontogeny. Mandibles were chosen to study dental innervation patterns because they are composed by a single bone (dentary) enclosing the IAN and the IAA. The mandibular canal soft tissues enter in a continuous canal posterior to the tooth

row and project anteriorly to its anterior end. Compared to the cranium, all branching patterns of the mandibular canal are therefore more easily traceable. The mandible is, therefore, a simpler model to study innervation patterns with the techniques used for this manuscript.

Acquisition of data

The studied specimens belong to the following collections: Natural History Museum, London (BMNH); Muséum National d'Histoire Naturelle, Paris (MNHN); Museum für Naturkunde, Berlin (ZMB); University Museum of Zoology, Cambridge (UMZ); Institut des Sciences de l'Evolution, Montpellier (ISEM); Museum of Vertebrate Zoology, Berkeley (MVZ); Louisianna State University Museum of Zoology (LSUMZ); United States National Museum (USNM); L.H. personal collection. High-resolution microtomography (µCT) was performed at Montpellier Rio Imaging (MRI; Microtomograph RX EasyTom 150, X-ray source 40-150 kV) platform, Imaging Analysis Center (BMNH; Nikon Metrology HMX ST 225, X-ray source 225 kV), and the Helmholtz Zentrum Berlin (HZB, Hamamatsu L8121-3, X-ray source 40-150 kV). The scan resolution differed according to the size of specimens (Table S1). Eight specimens were obtained from MorphoSource (www.morphosource.org), one from Digimorph (www.digimorph.org), and one from the Digital Morphology Museum (www.dmm.pri.kyoto-u.ac.jp). The left hemi-mandibles (the right one was used if the left one was missing or broken) were reconstructed, with respective mandibular canals and teeth. Avizo 9.4.0 (Visualization Sciences Group) was used to perform the 3D reconstructions. When teeth were absent, the mental branches were distinguished from the dorsal canaliculi by their larger diameter and their lateral projection to the mental foramina on the lateral aspect of the mandible [5,7]. Dorsal canaliculi were defined as dorsal projections of the mandibular canal opening on the dorsal surface of the mandible.

Histology

We also dissected the head of an adult specimen of *T. tetradactyla* (ISEM 778N) fixed in formalin. The right mandible was extracted and its associated musculature removed. The mandible was then subjected to decalcification during forty five days, following standard protocols. A portion of the mandible was then cut (as shown in Figure 4*A*) with the use of a scalpel, and fixed in paraffin. Serial slicing was performed to produce 3µm thick coronal and sagittal sections of the mandible. Luxol Fast Blue (LFB) was used to stain the slices in order to allow for the blue staining of the myeline sheaths insulating nerve cell axons. The LFB staining protocol was composed of several phases (1-11) in which acetic acid (10%), Luxol Fast Blue (0.1%), lithium carbonate (0.05%), and cresyl violet (0.1%) were used. (1) Histological sections were placed in a sealed container with the Luxol Fast Blue solution and were left overnight inside an oven at 58°C; (2) Sections were rinsed with ethanol (96%); (3) Sections were rinsed with distilled water; (4) Sections were differentiated in a lithium carbonate solution during 30 seconds; (5) Sections were placed in a rack with ethanol (70%) and were then stirred manually twice during periods of 15 seconds; (6) Sections were placed in a rack with distilled water and were then stirred manually during one minute; (7) A counterstain was performed by placing the sections in a cresyl violet solution during ten minutes; (8) Samples were quickly rinsed twice with ethanol (96%); (9) Sections were placed on ethanol (100%) for two periods of two minutes each; (10) Sections were placed on xylene (dimethylbenzene) for the same duration as in step (9); (11) Sections were mounted with a resinous medium (Pertex). A histological slice of a coronal section of the mandible of *Balaena mysticetus* (provided by J.G.M. Thewissen [22]) was used for anatomical comparisons (Figure S3*A*).

Supplemental item titles

Data S1. Supplemental Text for anatomical descriptions, histological comparison of the anteater and the bowhead whale, intraspecific variation, Vermilingua ancestral tooth pattern, and ancestral state reconstruction of the internal anatomy of the mandible. Related to Results and Discussion.

Table S1. Resolution of the performed µ-CT scans and scanning platform information. Related to STAR methods.

KEY RESOURCES TABLE

RESOURCE	SOURCE	IDENTIFIER
Biological Samples		
Proteles cristatus	This paper	BMNH 34.11.1.5
Canis lupus	https://www.morphosource.org/Detail/SpecimenDetail/Show/specimen_id/2716	LACM 23010
Manis crassicaudata	This paper	BMNH 67.4.12.298
Manis javanica	This paper	BMNH 9.1.5.858
Orycteropus afer	This paper	BMNH 27.2.11.113
Potamogale velox	This paper	ZMB 71587
Tenrec ecaudatus	This paper	Martinez pers. coll.
Rhynchocyon petrsi	This paper	BMNH 55.149
Procavia capensis	https://www.morphosource.org/Detail/SpecimenDetail/Show/specimen_id/5258	UMZC H4980K
Cyclopes didactylus	This paper	MNHN 1986-1115
Cyclopes didactylus	This paper	BMNH 24.12.4.68
Tamandua tetradactyla	This paper	BMNH 34.9.2.196
Tamandua tetradactyla	This paper	ISEM 788N
Tamandua tetradactyla	This paper	MVZ 153482
Myrmecophaga tridactyla	This paper	ISEM 071 N
Myrmecophaga tridactyla	This paper	ISEM 065 V
Myrmecophaga tridactyla	This paper	MVZ 185238
Bradypus tridactylus	This paper	ZMB 18834
Bradypus tridactylus	This paper	MNHN 1999-1065
Choloepus didactylus	This paper	ZMB 4949
Choloepus hoffmanni	This paper	Hautier pers. coll.
Dasypus pilosus	This paper	ZMB 19240
Dasypus novemcinctus	This paper	USNM 033867
Dasypus novemcinctus	This paper	LSUMZ 8538
Dasypus novemcinctus	This paper	LSUMZ 29160
Dasypus novemcinctus	This paper	BMNH 11.10.27.3
Dasypus novemcinctus	This paper	ZMB 84-357
Dasypus novemcinctus	This paper	USNM 020920
Priodontes maximus	This paper	ZMB 47528
Tapirus indicus	http://dmm.pri.kyoto-u.ac.jp/dmm/WebGallery/dicom/dicomProperty.html?id=506	KUPRI 506
Molossus molossus	https://www.morphosource.org/Detail/MediaDetail/Show/media_id/19283	AMNH 234923
Talpa europaea	This paper	Martinez pers. coll.
Cynocephalus volans	https://www.morphosource.org/Detail/MediaDetail/Show/media_id/18020	FMNH 56521
Lemur catta	https://www.morphosource.org/Detail/MediaDetail/Show/media_id/647	DPC-O92
Tupaia montana	https://www.morphosource.org/Detail/MediaDetail/Show/media_id/13025	FMNH 108831
Lepus europaeus	https://www.morphosource.org/Detail/MediaDetail/Show/media_id/23932	DMET-LE1

Rattus norvegicus	https://www.morphosource.org/Detail/MediaDetail/Show/media_id/28785	HACB-RN1
Dasyurus hallucatus	http://digimorph.org/specimens/Dasyurus_hallucatus/	TMM M-6921
Reagents		
Acetic acid	Merck	537020
Distilled water	Aguettant	3293
Luxol Fast Blue	Georges T. GURR	B2580
Lithium carbonate	Diapath	M00188
Cresyl violet	Merck	5235
Software and Algorithms		
Avizo 9.4.0	FEI	https://www.fei.com/software/amira-avizo/
Other		
Voxel size used for 3D model segmentation	This paper	Data S1

Figure 1

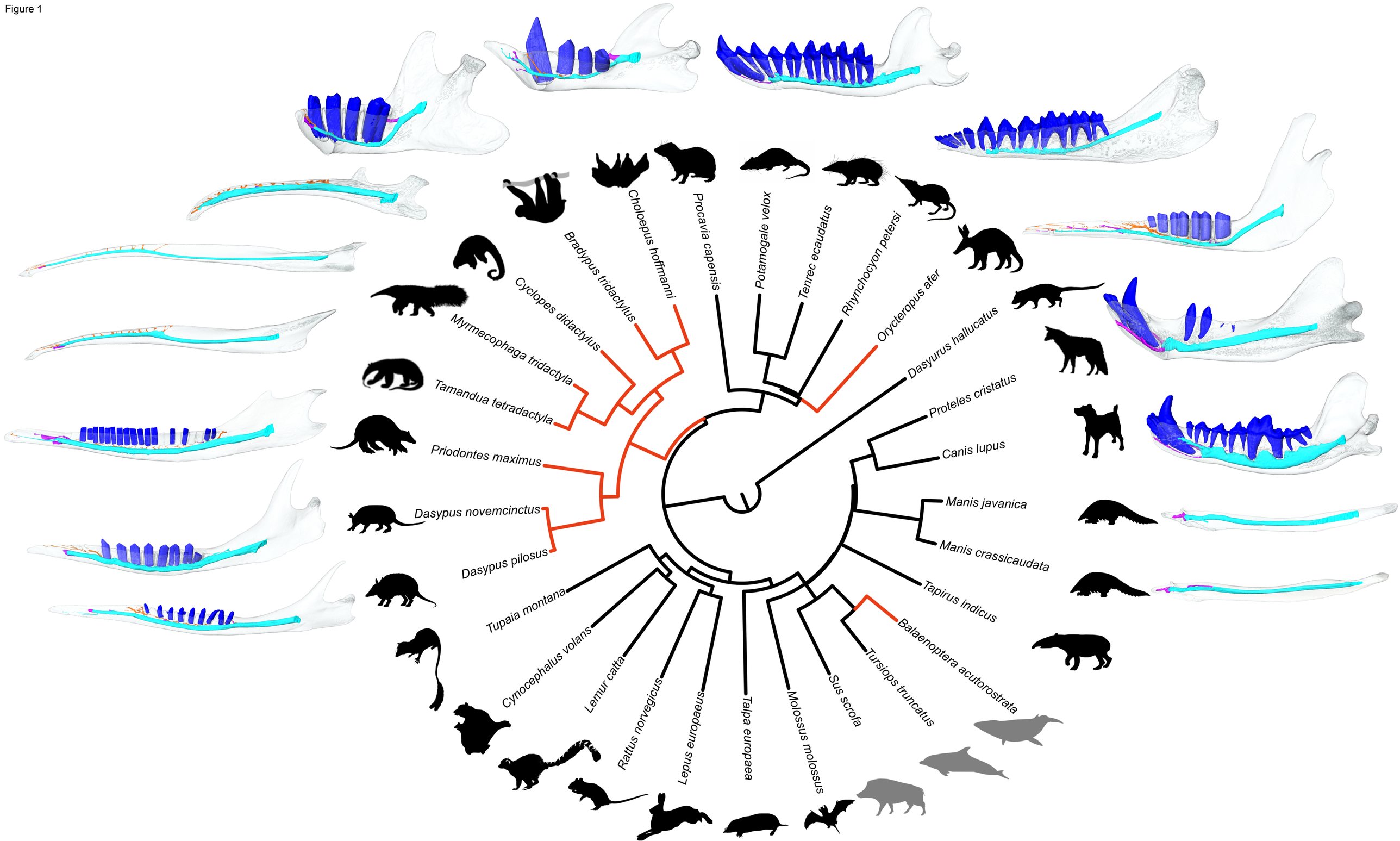
Choloepus hoffmanni
Procavia capensis
Potamogale velox
Tenrec ecaudatus
Rhynchocyon petersi
Orycteropus afer
Dasyurus hallucatus
Proteles cristatus
Canis lupus
Manis javanica
Manis crassicaudata
Tapirus indicus
Balaenoptera acutorostrata
Tursiops truncatus
Sus scrofa
Molossus molossus
Talpa europaea
Lepus europaeus
Rattus norvegicus
Lemur catta
Cynocephalus volans
Tupaia montana
Dasypus pilosus
Dasypus novemcinctus
Priodontes maximus
Tamandua tetradactyla
Myrmecophaga tridactyla
Cyclopes didactylus
Bradypus tridactylus

Figure 2

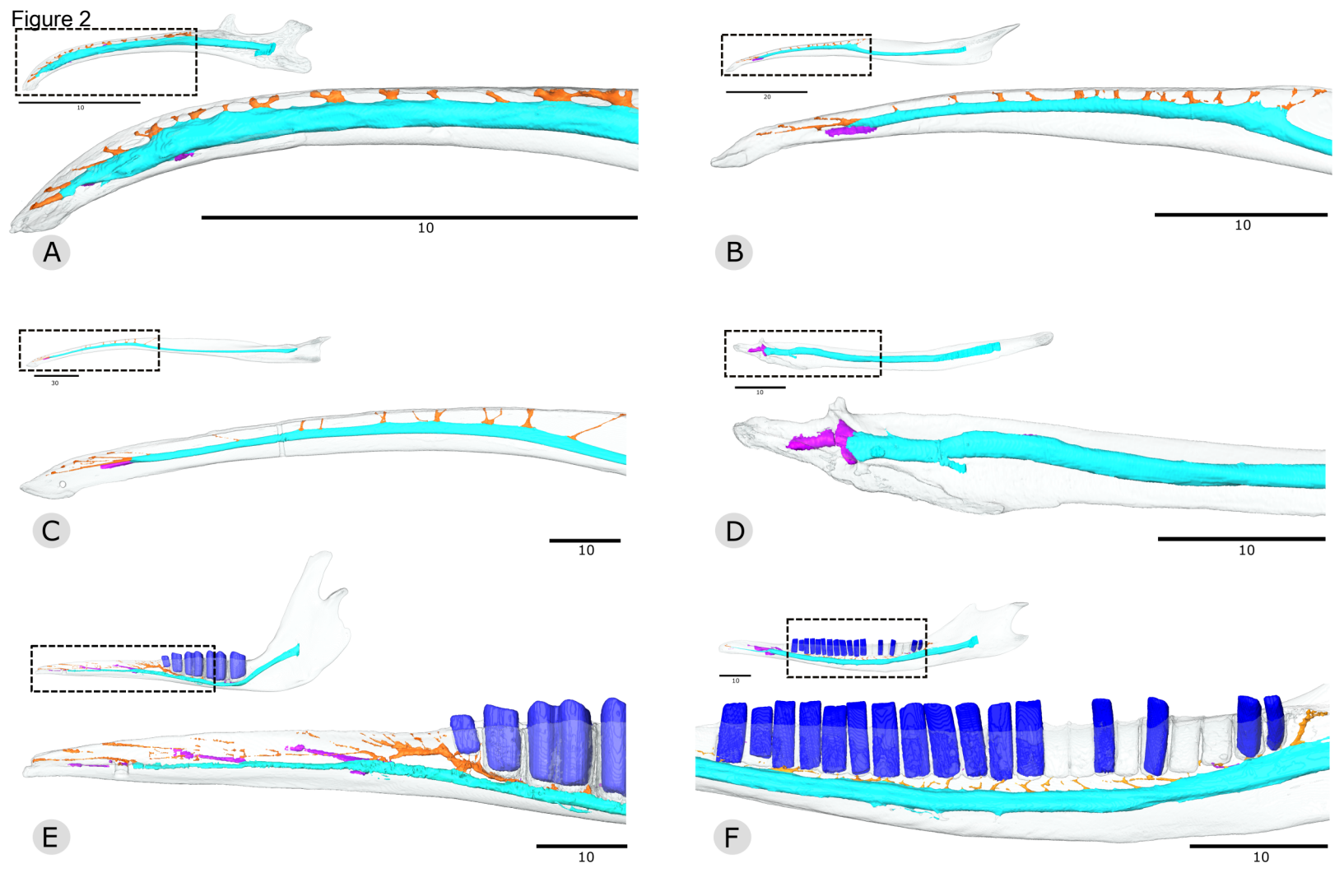

Figure 3

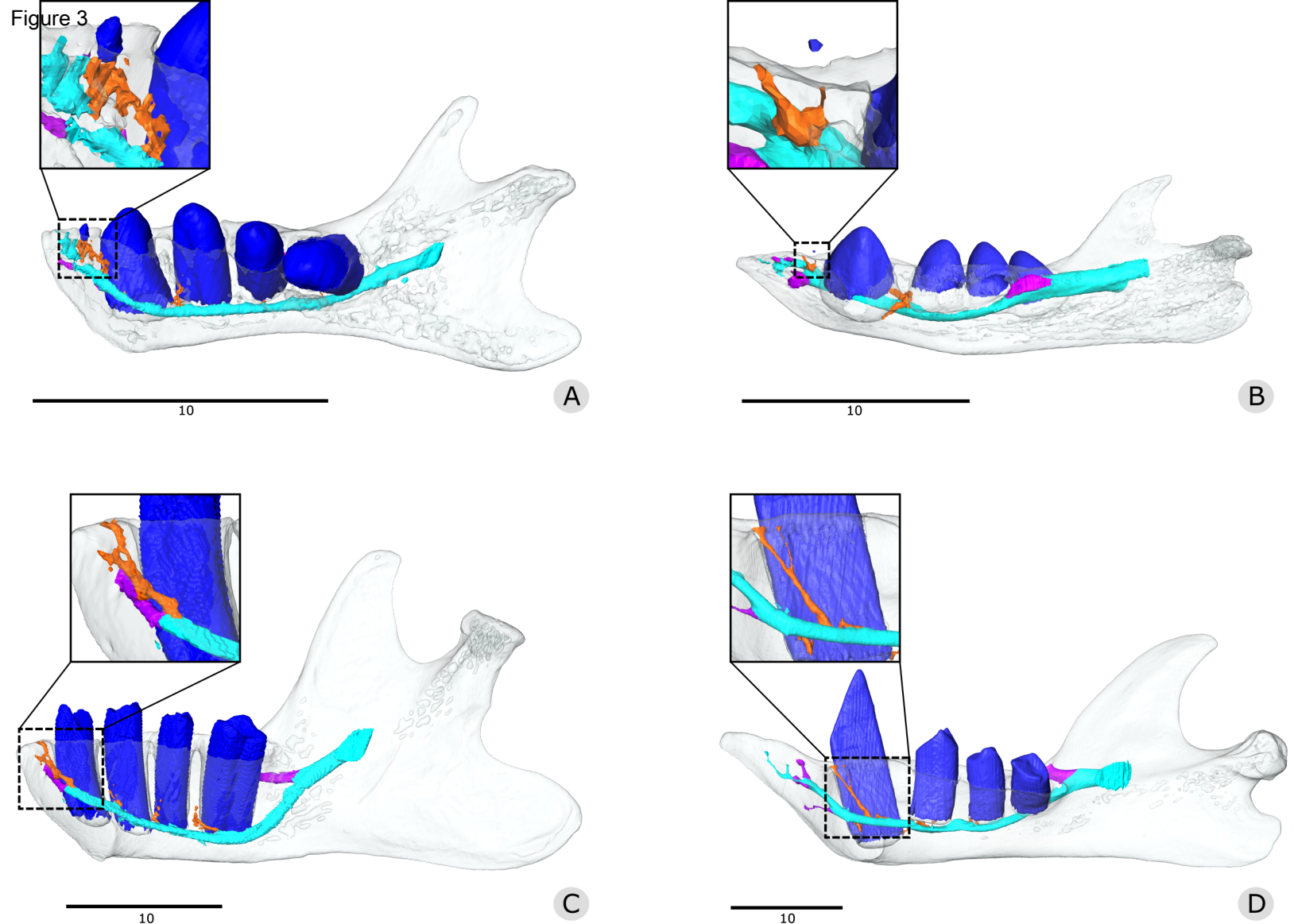

Figure 4

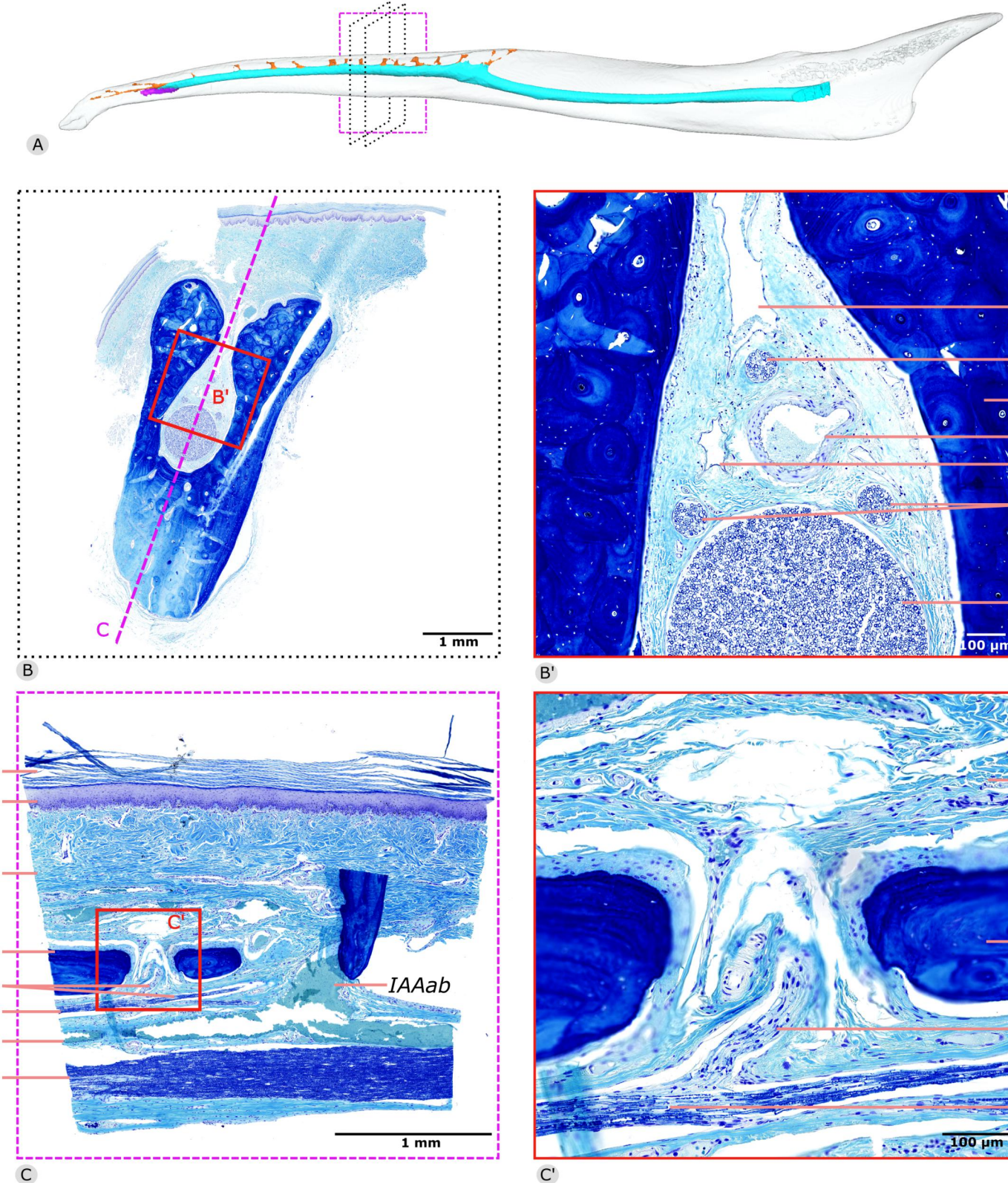
A
B'
C
1 mm
B
IAVab
IANa
bo
IAA
IAV
IANa
IAN
100 µm
B'
pa
ep
de
bo
IANab1,2
IANa
IAA
IAN
C'
IAAab
1 mm
C
de
bo
IANab
IANa
100 µm
C'

Evolutionary tinkering of the mandibular canal linked to convergent regression of teeth in placental mammals

Sérgio Ferreira-Cardoso[1,*], Frédéric Delsuc[1,3] and Lionel Hautier[1,2,*]

Author list footnotes

[1]Institut des Sciences de l'Evolution de Montpellier (ISEM), CNRS, IRD, EPHE, Université de Montpellier, Montpellier, France.

[2]Mammal Section, Life Sciences, Vertebrate Division, The Natural History Museum, London, UK

[3]Lead contact

[*]Correspondence: sergio.ferreira-cardoso@umontpellier.fr and lionel.hautier@umontpellier.fr

Supplemental information:

Supplementary text S1

1. Anatomical descriptions of myrmecophagous mammals and sister taxa

Pygmy anteater (*Cyclopes didactylus*)

The mandible of *Cyclopes didactylus* is low and slender. In lateral view, the horizontal ramus is thin, elongated and is highly curved with a ventral concavity, which makes it distinctive from all other anteaters. The ascending ramus is extremely inclined laterally, with the hook-like coronoid process projecting laterally. The mandible presents seven mental foramina (Figure S1*A*). We here designate the flattened part of the horizontal ramus of the mandible as the dentary pad. This dentary pad extends from the most anterior tip of the mandible to the posterior end of the coronoid process. This pad displays several dorsal foramina with foramina for dorsal canaliculi 9 to 15 forming a continuous groove. Nineteen foramina are present on the left dentary pad, 20 on the right mandible.

The mandibular canal displays a straight trajectory until it reaches the dentary pad, from where it curves ventrally, accompanying the shape of the mandible. The mandible has an elliptic-like section, and the major axis rotates, in anterior direction, from an almost transversal plane parallel position to a coronal one. The mandibular canal is positioned dorsally. The size of the mandibular canal remains constant along the horizontal plane, and decreases towards the symphysis. The mandibular canal presents several dorsal canaliculi (dc), which connect dorsomedially with the opening foramina. In total, there are fifteen dorsal (eighteen on the right mandible) and seven mental branches. Some of the dorsal canaliculi bifurcate and vary in diameter, with dc14 and dc15 being the largest (Figure S1*A*). The first four dorsal canaliculi (dc1 to dc4) are

anterodorsally oriented, as well as dc12, dc13 and the anterior projections of the bifurcating canaliculi. The mental branches also vary in diameter, with the most anterior one (mb1) being, by far, the largest, but no specific trend observed.

Collared anteater (*Tamandua tetradactyla*)

In *Tamandua tetradactyla* the edentulous horizontal ramus is long, slightly curved ventrally, and gets gradually shallower postero-anteriorly. The dentary pad is more anterior, narrower in its most posterior part, and not as medially inclined as in *C. didactylus* (Figure S1*B*); it is perforated by 17 foramina (Figure S1*B*, dc 1-15); a small and shallow groove connects the most posterior ones. Only one anterior mental foramen is present (Figure S1*B*, mb1). The ascending ramus is rather shallow and presents incipient coronoid and angular processes; the condyloid process is posteriorly projected.

The mandibular foramen (mb1, Figure S1*B*) is parallel to the mandibular canal. The mandibular canal opens on the medial surface of the ascending ramus and projects anteriorly with a slight ventral inclination. It projects dorsally from the posterior edge of the dentary pad, as is typical of toothed mammals after tooth loss [S1,S2]. Similarly to *C. didactylus*, dorsal canaliculi are present. Each quadrant presents 15 dorsal canaliculi; only dc1 and dc15 are bifurcated (Figure S1*B*). The canals of the dorsal canaliculi are relatively narrower than those observed in *C. didactylus*. Although the most anterior canals (dc1 to dc6) are slightly anteriorly oriented, this trend is not present on the most posterior ones (dc7 to dc14), which display a more random inclination. The most posterior canaliculus (dc15) is posteriorly inclined. Dorsal canaliculi dc1 and dc2 are spatially and morphologically distinct from the remaining (Figure S1*B*), and highly anteriorly inclined. Dc1 is extremely elongated and splits into two parts anteriorly.

Giant anteater (*Myrmecophaga tridactyla*)

The mandible of the adult *Myrmecophaga tridactyla* is, in many ways, similar to that of *T. tetradactyla*. It is larger in size but presents the same general morphology, with the body being elongated, transversely compressed and lacking teeth, and the ascending ramus being extremely simplified when compared to toothed xenarthrans. As in *T. tetradactyla*, the anterior part of the mandible is slightly curved, with the anterior tip tapering ventrally. A dentary pad occupies more than half of the total length of the jaw (Figure S1*C*), which is narrow posteriorly. Sixteen foramina are present on the dentary pad, and correspond to the dorsal opening of the dorsal canaliculi. Two mental foramina are present in the anterior part of the mandible, with the most anterior one (mb1, Figure S1*C*) opening laterally at the level of dc4 and the second one (mb2, Figure S1*C*), much smaller, opening at the level of dc5.

The mandibular canal opens in the medial surface of the ascending ramus, just dorsally to the position of the coronoid process, with an aperture with a long antero-posterior axis. A groove runs anteriorly along the canal. The latter gradually descends along the lengthy horizontal ramus, until it reaches the level of the posterior margin of the dentary pad (Figure S1*C*). It then projects dorsally to reach the level of dc5, from where it maintains its position in the mandible until it opens to the mental foramen (mb1), anteriorly. Along this path, thirteen main dorsal canaliculi open dorsally in the dentary pad. Dc13, the longest and most posterior dorsal canaliculus projects postero-dorsally. Dc12 to dc6 project dorsally, with some dorsal canaliculi displaying a simple column shaped, while others bifurcate dorsally. Dc5 is anteriorly inclined and has a much reduced diameter. Close to the symphysis, the first five dorsal canaliculi (dc1-5) form a distinct complex of long and anteriorly inclined canaliculi, similar to *T. tetradactyla*. In summary, the morphology of the mandibular canal of *M. tridactyla* is similar to *T.*

tetradactyla, except for the dorsoposteriorly oriented dorsal canaliculus (i.e. 13), and for the larger number of dorsal canaliculi on the anterior complex.

A juvenile specimen (ISEM - 071 N) was also analysed to check on the number of dorsal canaliculi. There are 16 dorsal canaliculi on the left side and 18 dorsal canaliculi on the right hemi-mandible. The posterior part of the mandibular canal is not well ossified and the division between branches is less clear. The posteriormost dorsal canaliculus is long and posteriorly projecting and does not reach the top of the mandible.

Indian pangolin (*Manis crassicaudata*)

The mandible of *Manis crassicaudata* is greatly compressed transversely and shallow. The ascending branch lack a true coronoid process as consists of a slightly dorsally inclined posterior knob-like projection. Three mental foramina (Figure S1*D*, mb1-3) are present on the anterior part of the horizontal ramus.

The mandibular foramen is antero-posteriorly elongated and has an anterior position in the ascending ramus. The mandibular canal projects anteriorly in a straight trajectory, near the dorsal margin of the mandible. From about the middle of the horizontal ramus the mandibular canal trajectory accompanies the dorsal edge mandible. This contrasts with anteaters, in which the mandibular canal position is ventral until it drifts dorsally at the posterior part of the dentary pad. The transversal section of the canal varies between a circular and an oval shape. From its most posterior part, the canal displays several small canaliculi that depart from the main mandibular canal, parallel to it. These parallel canaliculi are present around the mandibular canal, along its entire length, both dorsally and ventrally. Their density is higher on the anterior half of the horizontal ramus and the posterior part of the ascending ramus. On the anterior part of the mandible, the dorso-laterally projecting pseudo-tooth displays a small foramen for a parallel canaliculus and the very anterior tip of the horizontal ramus presents two of

these canaliculi. Most parallel canaliculi show no connection to the mandibular canal and only a few open in microscopic foramina (Figure S1*D*). The most posterior mental branch (Mb3) is short and opens in an elongated foramen just before it bifurcates. The remaining two mental foramina (associated to mb2 and mb3) open laterally close to the sharp anterior tip of the mandible. The small mb2 splits posteriorly to the pseudo-tooth while the large and elongated mb1 drifts laterally at the level of this prong.

Malayan pangolin (*Manis javanica*)

The mandible in *Manis javanica* is shallower than in *M. crassicaudata*. It presents five anterior mental foramina (Figure S1*E*, mb1-5), with the second most anterior (mb2) being clearly larger than the remaining ones. Between the posterior end of the symphysis and the pseudo-tooth, two small circular foramina open medially (Figure S1*E*).

The mandibular foramen in *M. javanica* differs from *M. crassicaudata*; it displays an elliptical shape with an extremely elongated antero-posterior axis. The dorsal and ventral margins of the foramen fade posteriorly and its internal surface becomes continuous with the medial surface of the ascending ramus.

Similar to its sister taxon, *M. javanica* displays a mandibular canal that presents a rather homogeneous shape and position along its path. Posteriorly, it slightly descends accompanying the inclination of the mandibular foramen and follows the general shape of the dorsal margin of the horizontal ramus until it reaches the mental foramina. The transversal section of the mandibular canal becomes slightly dorso-ventrally compressed at mid-length, but immediately assumes its former shape anteriorly. As described for *M. crassicaudata*, several parallel canals are present along the entire length of the mandible. The density of these small canals is particularly high in the anterior portion of the mandible as well as in the posterior part, at the level of the mandibular foramen.

Their morphology is in all aspects similar to the structures observed in *M. crassicaudata*, including the presence of a couple of vertical canaliculi that project dorsally and open through two small foramina in the pseudo-tooth, as well as the presence of a couple of canaliculi that reach the mandible surface in all directions. The mandible presents five mental branches: the three more posterior ones (Figure S1*E*, mb3-5) are short and small, and open laterally in small elliptical foramina posterior to the pseudo-tooth; the largest mental branch (Figure S1*E*, mb2) drifts antero-laterally to form a short branch at the level of the prong, opening in a large diamond shaped foramen; the most anterior mental branch (Figure S1*E*, mb1) represents the last remaining part of the main mandibular canal that projects anteriorly and opens just ahead of mb2 in an low and antero-posteriorly elongated foramen anterior to the pseudo-tooth.

Nine-banded armadillo (*Dasypus novemcinctus*)

Dasypus novemcinctus displays a thin, low and elongated horizontal ramus and a slightly broader ascending ramus characterized by its high and slender coronoid process. Anteriorly, the mandible is extremely low and transversely compressed, and displays a short symphysis. It is higher posteriorly and becomes transversely wider at the level of the tooth row. The dental formula is c 1, p 7, m 1. The anterior quarter of the mandible is completely toothless but an alveolus for a canine [S3,S4] is visible at the level of the first mandibular foramen (Figure S1*F*, mb1), and is separated from the rest of the tooth row by a small diastema. The molar is not erupted. This specimen displays two mental foramina: the most posterior one (mb2) is located between the second and the third premolars while the anterior one (mb1) opens anteriorly to p 1.

Below the anterior edge of the coronoid process, a slightly elongated mandibular foramen opens on the medial surface of the ascending ramus, at roughly the same height of the alveoli. It projects ventrally with an inclination of around 14° until the

posterior end of the tooth row. The canal describes a shallow dorsal facing concavity contouring the alveoli ventrally and accompanying the curvature of the ventral edge of the horizontal ramus. Immediately anteriorly to the third premolar, a slightly antero-dorsally inclined posterior mental foramen is present on the medial side of the mandible. Anteriorly to the first molar, the main branch of the mandibular canal opens laterally in an antero-posteriorly elongated mental foramen. This foramen is particularly large and elongated. Anteriorly to the first molar, a dorsal canaliculus with a rather large diameter is also oriented antero-dorsally in the direction of the alveolus for the canine. The canaliculus opens in the alveolus and continues anteriorly – with less than half the diameter – to split into two ramifications. The most posterior ramification bifurcates just dorsally to mental foramen 1 and opens into two small foramina (Figure S1*F*, dc 1c,d) on the dorsal margin of the mandible. The anterior ramification (dc 1a,b) describes a long trajectory antero-ventrally to dc 1c,d, and bifurcates near the anterior tip of the mandible. All bifurcation of the dorsal canaliculus (dc 1a,b,c,d) open into tiny foramina on the dorsal side of the mandible.

In a juvenile specimen (USNM 020920), the canal does not open directly into the first five premolars and the canine. Therefore, the juvenile mandible displays longer dorsal canaliculi for the premolar dentition than the adults. A large dorsal canaliculus is associated to the first molar, which is absent. Anterior to the canine, a dorsal canaliculus projects anterodorsally, splitting in a plexus of three smaller canaliculi that open dorsally in three individual foramina. The dorsal canaliculi pattern is similar to the one observed in adults.

Hairy long-nosed armadillo (*Dasypus pilosus*)

The anterior part of the slender mandible is sharp and its height slightly increases at mid-length of the horizontal ramus. A row of rather spaced peg-like teeth occupies the

second third of the mandible. *D. pilosus* presents a c 1, p 7, m 1 lower dental formula. The c1 and m1 present a basic peg-like shape. The anterior four mental foramina are positioned between the p 3 and the margin of the most anterior and largest mental foramen (Figure S1*G*, mb1), at the level of the fused symphysis. The most posterior and smallest of the five mental foramina is located posterior to the m 1 alveolus.

The symphysis is elongated, reaching the level of the anterior margin of mb1. The mandibular canal is ventrally positioned at the level of the alveolar portion of the mandible. The canal opens posteriorly in a high mandibular foramen and extends ventrally towards the centre of the tooth row at the level of the fourth premolar. From this point it projects slightly dorsally, accompanying the shape of the mandible, until the level of mental foramen 3. Anterior to mb3, the mandibular canal presents a straight trajectory. Immediately dorsal to the mandibular canal, the horizontal ramus displays a small canal that originates in the p 6 alveolus and passes through all alveoli until p 2. From this point it projects antero-dorsally, as a dorsal canaliculus, to reach the p 1 alveolus. From this alveolus it projects further antero-dorsally to the c 1 alveolus and extends in the same direction until the level of third mental foramen. This dorsal canaliculus presents a bifurcation anterior to c 1 (Figure S1*G*). A second dorsal canaliculus arises at the level of mental foramen 3, bifurcating and ending just anteriorly. Neither of these canaliculi reaches the dorsal margin of the mandible. No foramina open in the anterior part of the mandible, close to the symphysis.

Giant armadillo (*Priodontes maximus*)

The mandible is long and displays a long tooth row extending for about half its total length. Similarly to *D. novemcinctus* and *D. pilosus,* the mandible is narrow, transversely compressed, although it is slightly more robust. As in anteaters, this mandible presents a medio-lateral rotation anteriorly. The left tooth row is composed of 22 hypselodont teeth,

23 on its right counterpart. In lateral view, three mental foramina (Figure S1*H*, mb 1-3) can be observed just anterior the tooth row. A fourth small one is present in the same area, but appears to be an extra branching of mental foramen (mb1) with no symmetrical branch on the right hemi-mandible.

The transversely compressed mandibular canal of *P. maximus* exhibits some differences compared to the other genus of armadillo here studied. The mandibular foramen is dorsoventrally elongated as in *Dasypus* but its position is more dorsal in the ramus when compared to the alveolar plane. The canal extends ventrally with a weak inclination (~12.2°). Posterior to mf 22, a large dorsal canaliculus (Figure S1*H*, dc3), slightly inclined posteriorly, projects dorsally and opens into several small foramina. Anteriorly, although alveoli for mf 1 and mf 2 are almost adjacent to the canal, small dorsal canaliculi are visible. As the canal projects ventrally towards alveolus for mf16, the dorsal canaliculi become longer. Their morphology varies, being anteriorly oriented and sometimes bifurcated. These canaliculi vary in diameter and can bifurcate (e.g., below alveolus for mf 17 and mf 18, Figure S1*H*), with a branch projecting dorsally and the other anteriorly, to merge with the immediately anterior dorsal canaliculus. Anteriorly to alveolus of mf 16 the mandibular canal displays a parallel trajectory to the alveoli row until alveolus for mf 9. From this point, it projects dorsally until mental foramen 1, being positioned immediately ventral to the nine most anterior alveoli. Along its path to the symphyseal portion of the mandible, the mandibular canal displays several minor mental branches before it splits into three larger mental canals (Figure S1*H*, mb 1-3) anterior to the first alveolus. The most posterior and smaller mental branch splits from the main canal right anteriorly to alveolus for mf 1, projecting anterodorsally and then drifting laterally. A second larger mental branch (mb2) splits anteriorly, departing from the dorsolateral part of the mandibular canal and opening in an antero-posteriorly elongated foramen. The most anterior and largest mental branch (mb1) also opens into an antero-

posteriorly elongated foramen. A more anterior small branch is visible on the lateral side of the mandible, but corresponds to a small ramification of the largest mental branch (mb1). Another canaliculus of the mandibular canal, which splits from the posterior part of the mb1, continues anteriorly toward the antero-dorsal end of the mandible. This small canaliculus (dc1) divides into three smaller ramifications, which open on the medial side of the anterior tip of the mandible.

Aardwolf (*Proteles cristatus*)

Proteles cristatus displays a mandible with a relatively high horizontal ramus displaying an anteriorly projected anterior margin. The specimen displays the following dental formula: i 3, c 1, p 2, m 2. This mandible displays three mental foramina (Figure S1*I*, mb1-3), with the first and second mental foramina displaying oval apertures of similar size. The first mental foramen is located on the anterior margin of the mandible and the second one is anterior to the canine, below the anterior end of the diastema. The third mental foramen is located below the diastema, half way through the height of the mandible.

The mandibular foramen is oval shaped, located in the middle of the ascending ramus, antero-ventral to the dorsal tip of the coronoid process. The mandibular canal has an oval section, being noticeably dorso-ventrally elongated from the anterior end of the coronoid process to the level of the m 1. The mandibular canal projects slightly ventrally until the posterior limit of the diastema. None of the four check teeth alveoli is adjacent to the mandibular canal. The first and second molars are dorsally placed relative to the canal; no dorsal canaliculus reaches their alveoli. The inferior alveolar nerve and artery branches reach the teeth through the many hollow cavities of the alveolar portion of the mandible. The trabecular nature of the molar area is particularly evident anteriorly (Figure S1*I*), dorsally and posteriorly to the premolar alveoli, almost

285 reaching the dorsal edge of the mandible. Posteriorly, fused trabeculae form a sort of
286 posteriorly projecting canals, which reach the dorsally placed m 1 and m 2 alveoli.
287 Anterior to the c, below the diastema, three mental branches (Figure S1*I*, mb1-3) split
288 and project antero-dorsally. Mb3 projects dorsally and opens laterally right ventrally to
289 the midpoint of the diastema. Mb2 projects antero-dorsally and is laterally inclined,
290 opening latero-ventrally to the canine. Mb1 is long and projects antero-dorsally, passing
291 through the middle of i 2 and i 3 and opens in the anterior margin of the mandible.
292
293 **Dog (*Canis lupus*)**
294 *Canis lupus* presents a mandible with a high ascending ramus, with a relatively broad
295 coronoid process. The mandible presents 11 tooth loci (i 3, c 1, p 3, m 3) and contrasts
296 with *P. cristata* in its complete tooth row (no diastema), its shorter symphysis and rather
297 vertical anterior margin. Four mental foramina are present (Figure S1*J*, mb1-4). The first
298 mental foramen opens anteriorly, ventral to i 2. The second and largest mental foramen
299 opens laterally between p 1 and c 1. The third mental foramen opens at the level of the
300 anterior root of p 3 and the fourth mental consists of a rather small lateral aperture
301 located between the ventral tips of the anterior and posterior roots of p 4 and p 3,
302 respectively.
303 The mandibular foramen resembles *P. cristata*, yet the canal projects slightly
304 more ventrally. Just posteriorly to the anterior edge of the coronoid process, the
305 mandibular canal becomes more extended anterodorsally (Figure S1*J*), displaying a
306 pseudo elliptical cross section. This is a main characteristic of the mandibular canal of
307 the dog. With the exception of m 3, teeth are rooted deeply enough to be in close
308 contact with the dorsal edge of the mandibular canal. The trajectory of the mandibular
309 canal follows the shape of the ventral margin of the mandible from the level of the
310 posterior root of m 1 until p 2, where it branches (Figure S1*J*). The large m 1 is so deeply

311 rooted that both its roots protrude ventrally into the mandibular canal. Along its
312 trajectory, the mandibular canal is topped by a complex of trabeculae that surrounds the
313 tooth roots. From about the second m 1 cusp, the mandibular canal gradually decreases
314 in height anteriorly. All but the small fourth mental branch project anterolaterally. Mb4 is
315 a very thin branch that projects posterolaterally below the posterior edge of p 3. Mb3 is
316 comparatively larger and splits from the mandibular canal just ventrally the anterior root
317 of p 3. Mb2 is large in diameter and projects anterolaterally ventrally to p 2 to open in an
318 oval-shaped foramen between p1 and c (Figure S1*J*). Mb1 is a rather thin and extremely
319 long ramification of the mandibular canal that projects anteriorly to pass dorsally to the c
320 and i 1-3 roots and open in the anterior margin of the horizontal ramus. In its trajectory,
321 mb1 opens to the alveolus of i 3. Dorsally to the branching point of mb1, a relatively
322 large accessory branch of the mandibular canal projects anterodorsally. This branch is
323 medially oriented and almost reaches the symphysis, posterior to which it divides into
324 several trabeculae.
325
326 **Pale-throated three-fingered sloth (*Bradypus tridactylus*)**
327 In the adult *Bradypus tridactylus*, the mandible is characterized by a short but robust
328 horizontal ramus, bearing one caniform (Cf) and three molariform teeth (mf 1-3), and a
329 high ascending ramus. The tooth row almost occupies the entire length of the body of
330 the mandible, with teeth inclination becoming more medial along the antero-posterior
331 axis. All four teeth are tall, lack roots and are deeply rooted in the mandible. The
332 mandible presents two mental foramina with one at the anterior tip of the mandible
333 (Figure S1*K*, mb 1) and a larger one at the level of the mf 4 (Figure S1*K*, mb2).
334 The morphology of the mandibular canal is very distinct from that observed in
335 anteaters and armadillos. The mandibular foramen is elliptical in shape, with the major
336 axis oriented anteroposteriorly with a similar inclination to the condylar process. The

canal projects antero-ventrally from the mandibular foramen until it reaches its lowest position in the mandible, at the level of the mf 3 At the same level, but higher in the body of the mandible, the largest and most posterior mental branch opens on the lateral side of the mandible, after branching midway between the mandibular foramen and the lowest mandibular canal position. The mandibular canal then runs anteriorly and gradually projects dorsally in the mandible until it reaches mental foramen 1. There is one small dorsal canaliculus (dc 1-3) for each of mf 1, mf 2 and mf 3. Dc4 is originates ventrally to mf3 but extends anterodorsally to reach the alveolus on its anterior margin. The mandibular canal runs medial to the first tooth and divides into dorsal and mental branches. The mental branches follow the same direction and inclination as the main branch and eventually reach the anterior tip of the mandible, lateral to the symphysis. The dorsal canaliculus assumes a steep trajectory (roughly parallel to the anterior margin of the mandible) and exits the mandible dorsally. This dorsal canaliculus likely corresponds to a remnant of the innervation/vascularization of an additional tooth locus identified in a previous work [S5] and opens anteriorly to alveolus for Cf. The juvenile specimen (ZMB 18834) displays a vestigial tooth in the same position; its mandibular canal of the foetus presents a similar general morphology, differing in number of mental and medial branches. The foetal mandible presents four foramina for accessory branches that open in the medial side of the mandible and four mental foramina. This mandible is much less ossified, compared to the adult.

Two fingered sloth (*Choloepus hoffmanni*)

The mandible of *Choloepus hoffmanni* presents shallower horizontal and ascending rami compared to *B. tridactylus*. The anterior tip of the horizontal ramus is shovel-shaped and elongated. The mandible bears three molariform teeth (mf 1-3) and one anterior caniniform tooth (cf). In total, the *C. hoffmanni* mandible presents four mental foramina,

363 a large one at the level of the root of the coronoid process and three small ones anterior
364 to the caniniform tooth.
365 Due to the differences in mandible shape, the morphology of the mandibular
366 canal is also different between the two sloth genera. Here again, the dorsal canaliculi of
367 the mandibular canal are present when the tooth alveoli are more dorsal. The canal
368 starts at the level of the dorsal edge of the horizontal ramus and runs anteriorly until it
369 reaches the level of the posterior margin of the tooth row. At this level, the mandibular
370 canal bifurcates, with a mental branch (Figure S1*L*, mb4) projecting antero-laterally to
371 open in a large mental foramen, just anteroventrally to the root of the coronoid process.
372 The main branch projects medially from the mandibular foramen, passing marginally
373 ventrolaterally to mf 3. A small dorsal canaliculus of the mandibular canal (Figure S1*L*,
374 dc 10) projects medially and allows for the innervation and vascularization of mf 3, which
375 is medially oriented. As the mandibular canal runs anteriorly, its position gradually
376 changes to a more medial one. This contrasts with the morphology of the mandible of
377 the adult *B. tridactylus*, in which the mandibular canal is medially positioned along the
378 entire length of the tooth row. Two dorsal canaliculi of the mandibular canal (df8-9) are
379 ventral to the anterior half of mf2. Three dorsal canaliculi (dc5-7) reach the alveolus for
380 mf 1. Dc5 is a small canal that splits at mid-lenght of the alveolus and joins the main
381 canal just anteriorly to it (Figure S1*L*). From this canal, three small dorsal projections
382 reach the alveolus. Two smaller additional innervation/vascularization canaliculi are
383 present posteriorly (Figure S1*L*, dc 6-7). Close to the symphysis, the mandibular canal
384 steadily projects dorsally. The main branch passes medially to the cf and, as in *B.*
385 *tridactylus*, its position is dorsal to the base of the alveolus. In fact, dorsal canaliculi
386 reach the alveolus of the cf. The more posterior canaliculus (Figure S1*L*, dc4) bifurcates
387 from the mandibular canal antero-ventrally just anterior to the alveolus for the cf.
388 Anteriorly, a small canaliculus (dc3) splits from the mandibular canal and projects

laterally into the same alveolus. The third canaliculus that connects to the alveolus of the cf (dc1) is located just anterior to the mandibular canal steep antero-dorsal projection in the direction of the anterior tip of the mandible. A long dorsal canaliculus (Figure S3*B*, dc2) splits from the mandibular canal in the direction of the rudimentary alveolus of the vestigial tooth that is observed on earlier ontogenetic stages. The vestigial alveolus, located just antero-medially to the anterior edge of cf, is also innervated/vascularized, with the dorsal canaliculus further splitting in two ventrally to its dorsal opening. Three small mental branches (Figure S1*L*, mb1-3) are present in the anterior part of the mandible: the most posterior (mb3) departs from the mandibular canal to open laterally at the level of mb2; mb2 projects dorsolaterally near the dorsal margin of the mandible; mb1 splits at about the same length as mb2, but projects anterolaterally. Anteriorly to the level of the foramen for mb1, a small branch (Figure S1*L*, ab) reaches the mandible shovel-shape projection and further divides into two small canals that open dorso-medially. These canals are not present in *B. tridactylus*.

The mandible of the foetus of *Ch. didactylus* (ZMB 4949) presents a lower level of ossification and allometric shape differences. Nevertheless, the mandibular canal of the foetus presents the same branch pattern as observed in the adult.

Aardvark (*Orycteropus afer*)

This mandible consists of a transversely compressed long and shallow horizontal ramus and a comparatively very high ascending ramus. The anterior half of the horizontal ramus is edentulous, while its posterior half presents three molars and two premolars (i 0, c 0, p 2, m 3; Figure S1*M*). The molars are large and deeply rooted and display an oblanceolate shape in dorsal view; the premolars are much smaller, transversely compressed, and are rooted more dorsally. The mandible of *Orycteropus afer* displays four major mental foramina (Figure S1*M*, mb1-4), with six small mental branches

laterally positioned compared to the tooth row (Figure S1*M*, mb5-10). A total of seven foramina for dorsal canaliculi are present. The anteriormost four foramina are aligned just anteriorly to p 5 (*sensu* [S6]; dc3). Another small foramen is present anteriorly, at the level of the third mental foramen (dc2). Two slightly larger and longer foramina open between mental foramina 1 and 2 (dc2). The most anterior foramen (dc 1) opens anteriorly in the middle of the anterior apical portion of the mandible. The dc1 foramen resembles the reticular alveolar foramen of whales [S7,S8].

The mandibular foramen is narrow and located well above the tooth row level, from where the canal projects ventrally. Between m 3 and m 1, the trajectory of the mandibular canal changes as it gradually projects dorsally, accompanying the height decrease of the horizontal ramus. The mandibular canal is adjacent to alveoli of m 1-3 and dorsal canaliculi are absent. From m 3 to p 5, only mental branches bifurcate from the mandibular canal (mb 5-10). The p5 and p6 alveoli are placed more dorsally in the mandible and are connected to the mandibular canal by two dorsal canaliculi, which project antero-dorsally. The two canaliculi dorsal to p 5 and p 6 (dc3 and dc4) are connected by a small canal parallel to the mandibular canal. Anterior to p 5, the main dorsal canaliculus (dc3) steadily extends dorsally, and then divides into four small canals linked to foramina dorsally. At the level of mb4, dc3 projects ventrally to merge with the mandibular canal, and a new dorsal canaliculus (dc2, Figure S1*M*) projects antero-dorsally. Dc 2 is long and presents a small diameter. It bifurcates three times: just anteriorly to its origin, a small ramification projects antero-dorsally to open at the level of mb4; the dorsal canaliculus continues anteriorly and bifurcates again between mb1 and mb2, with one branch projecting antero-dorsally but never opening dorsally; a thin branch of dc2 continues until it splits in several smaller canals near the third mental foramen, with one of them opening dorsally at the level of the second mental foramen. Mb2 and dc1 split near the anterior end of the mandibular canal. Dc1 bifurcates – with

441 one branch projecting antero-dorsally and the other anteriorly – before it opens in two
442 foramina. The most posterior branch of dc1 opens at the level of the second mental
443 foramen. The most anterior canaliculus reaches the anterior tip of the mandible, ending
444 in a foramen similar in position to the reticular alveolar foramen found in rorquals
445 [S7,S8].
446
447 **Giant otter-shrew (*Potamogale velox*)**
448 The mandible of *Potamogale velox* presents a relatively low horizontal ramus with a
449 rather long and anteriorly inclined symphysis. The ascending ramus of is high due to the
450 presence of a broad sub-triangular coronoid process. The tooth row is composed of ten
451 teeth (i 3, c 1, p 3, m 3). Three mental foramina are present in the mandible (Figure S1*N*,
452 mb1-3). The first mental foramen is small and opens on the anterior margin of the
453 mandible. The second and third mental foramina are relatively larger and open laterally
454 at the level of p1 and the posterior root of m1, respectively.
455 The mandibular foramen has a pseudo circular shape. Posteriorly, the
456 mandibular canal presents a slightly descending trajectory until it reaches the m 2. The
457 trajectory is then practically horizontal until the canine. Small complexes of trabeculae
458 are present dorsally to the mandibular canal. The trabeculae surround the tooth roots,
459 which are deeply implanted in the mandible. With the exception of the c and i 1-3, all
460 alveoli enter in contact of the mandibular canal. The most posterior mental branch
461 (Figure S1*N*, mb3) is the largest in diameter and projects laterally at the level of the tip of
462 m 1 posterior root and opens slight dorsally in an elliptical shaped foramen. At the level
463 of p 2, the trajectory of the canal drifts slightly dorsally, accompanying the small ventral
464 concavity of the ventral edge of the horizontal ramus. Two branches split from the
465 mandibular canal, dorsal to p 1, and project laterally. These branches merge into one
466 larger mental branch, opening laterally in a single foramen (Figure S1*N*, mb2). Mb1

consists of a rather long branch, small in diameter, which projects anteriorly (Fig S1*N*, mb1). This branch passes ventrally to c alveolus and gradually projects dorsally to open anteriorly, between i 2 and i 1. Two accessory branches of the mandibular canal split at the level of p 1 and c. The posterior one projects anterodorsally until it divides into a trabeculae complex at the level of i 3 and i 2 alveoli. The anterior one also projects anterodorsally but it meets the trabeculae briefly anteriorly to its branching point. This trabeculae complex is located medially in the mandible and is associated with the i 2 alveolus and the symphysis.

Anatomical description of additional taxa

A total of 12 species were segmented in order to reconstruct the phylogenetic history of the absence/presence of dorsal canaliculi (Figure 1). One Afrosoricida (*Tenrec eucaudatus*) and one Macroscelidea (*Rhynchocyon petersi*) were additionally segmented to increase the number of species with relatively close phylogenetic affinities to *Orycteropus afer* (Figure 1). Neither of the 12 species described in this section presents dorsal canaliculi. With the exception of the brown rat (*Rattus norvegicus*) and the velvet free-tailed bat (*Molossus molossus*), all the species present mandibular canals very similar in shape (Figure S2*A*-*I*). The mandibular foramen displays a descending trajectory anteriorly until the third molar (m 3). It projects anteriorly, ventrally to the tooth row, with its dorsal margin that usually opens directly to adjacent post-canine tooth alveoli (Figure S2). In some species (e.g., *Dasyurus hallucatus*, *Lemur catta*, *Cynocephalus volans*, or *Procavia capensis*; Figure S4*A*-D) a large amount of trabecular tissue is visible around the teeth, and connects the mandibular canal to the alveoli, only when both structures are not adjacent to each other. The Malayan tapir (*Tapirus indicus*, Figure S2*E*) constitutes the most remarkable case of innervation/vascularization via trabeculae, with a mandible characterized by non-adjacent tooth alveoli and mandibular

canal. In almost all species, an incisor branch projects anteriorly at the level of the most anterior mental branch, and usually splits into several trabeculae that wrap both canine and incisor teeth. In the rock hyrax (*Procavia capensis*), however, the incisor branch opens directly into the corresponding alveolus. The tailless tenrec (*Tenrec ecaudatus*, Figure S2*F*) also presents a slightly different morphology of the incisor branch, with the mandibular canal opening directly into the alveolus of the canine, with the latter being connected to the following alveolus. In the brown rat (*Rattus norvegicus*, Figure S2*K*) the incisor branch is absent, with the alveolus of the incisor tooth extending back into the ascending ramus of the mandible. The innervation/vascularization of the incisor tooth arrives ventral to the coronoid process, as the mandibular canal partially merges with the alveolus. Although the Malayan tapir exhibits a classical incisor branching of the mandibular canal, the latter differs in from other species by its extremely reduced diameter (Figure S2*E*). The overall shape of the mandibular canal of the brown rat is peculiar due to the extreme posterodorsal projection of the incisor alveolus (Figure S2*K*). The mandibular canal merges with the incisor alveolus medially, just anteriorly to the mandibular foramen. It projects anteriorly at the level of the m 3 and its trajectory follows the shape of the dorsal margin of the incisor alveolus. The mandibular canal opens directly to the m 3 and m 2. In the most anterior portion of the alveolar part of the mandible, which corresponds to the alveolus of the m 1, the mandibular canal presents a relatively ventral position relative to the first molar alveolus, the tooth being likely innervated/vascularized via trabecular bone. The mandibular canal opens dorsolaterally in a single mental foramen, just anteriorly to the m 1. The velvet free-tailed bat also presents a distinct mandibular canal morphology (Figure S2*L*). Compared to other species, the mandibular canal is unusually high. Here again, all pre-canine tooth alveoli are adjacent to the mandibular canal. However, the mandibular canal seems to extend dorsally, in between tooth roots (Figure S2). This might be a result of the scan resolution

519 compared to the reduced size of the specimen, for in other segmented placental
520 mammals, those spaces are normally filled with trabeculae (Figure S2). Apart from this
521 abnormal height, the mandibular canal of the velvet free-tailed bat resembles those of
522 other toothed species; it is positioned ventrally to the tooth row and bifurcates anteriorly,
523 with a mental branch that projects laterally while the other branch of the canal opens into
524 a trabecular system wrapping the canine and the incisors. An anterodorsally projecting
525 mental branch is also present and opens ventrally to the incisors, similar to the condition
526 observed in carnivores (Figure S2*D*, *E*).
527
528
529 **2. Homology of dorsal canaliculi between anteaters and baleen whales**
530 The trigeminal nerve originates in the pons and has two different roots, a sensory and a
531 motor root [S9]. The mandibular branch of the trigeminal is composed of both sensory
532 and motor roots and is designated by inferior alveolar nerve (IAN) [S9]. The nerve enters
533 the medial side of the mandible through the mandibular foramen, and is accompanied by
534 the inferior alveolar artery [S10]. Typically, the inferior alveolar nerve separates into four
535 types of branches [S9,S10]: the mylohyoid branch supplies the hyoid musculature; the
536 dental/inferior dental branches supply molars and premolars, each nerve branch
537 innervating one tooth; the incisor branch supplies canine and incisors. The mental
538 branch supplies the lip integument (the number of mental branches may vary between
539 taxa). Here, we will group dental and incisor branches to follow the nomenclature of
540 previous references for edentulous placentals [S7].
541 In *Tamandua tetradactyla*, the large inferior alveolar nerve (Figure 4*B'*, IAN) is
542 placed dorsally in the mandibular canal. Two accessory branches of the IAN (Figure 4*B'*,
543 IANa) are present dorsolaterally to the IAN. The inferior alveolar artery (Figure 4*B'*, IAA)
544 lies dorsally to the IAN. An irregularly shaped branch of the inferior alveolar vein (Figure

4*B'*, IAV) is placed laterally to the IAA. A third branch of the IAN (Figure 4*B'* and S3*B*, IANa) is visible dorsally to the IAA. Dorsally to it, the ascending branch of the IAV (Figure 3*B'* and S3*B*, IAVab) is present in the dorsal canaliculus of the mandibular canal. A keratinous dental pad covers the dorsal part of the mandible (Figure 4*C*, pa). Ventrally, the epidermis consists of a small layer (Figure 4*C*, ep) and, which lies dorsally to the thick dermis layer (Figure 4*C*, de). In addition to connective tissue, the dermis presents several blood vessels and small nerve branches. The most posterior dorsal canaliculus allows for the passage of an ascending branch of the IAN (Figure 4*C*,*C'*, IANab1); the anterior dorsal canaliculus displays a large ascending branch of the IAA (Figure 4C, IAAab) and likely features a second ascending branch of the IAN (Figure 4*C*, IANab2) that projects anterodorsally.

A histological section (coronal plane) of the mandible of a bowhead whale (*Balaena mysticetus*) showing the 15th vestigial tooth [S11] shows the mandibular canal and associated soft tissues (inferior alveolar nerve, blood vessels) with two small canals (Figure S3*A*, red squares) dorsally. The most dorsal small canal is most likely associated to the vestigial teeth observed in the figure, while the most ventral one is associated to the 14th vestigial tooth. Its position between the mandibular canal and the tooth row, plus the presence of branches of the inferior alveolar artery and the inferior alveolar nerve inside these small canals, highly suggest that these are homologous to the dorsal canaliculi observed in the collared anteater (*T. tetradactyla*). Dorsal canaliculi are anteriorly inclined in whales [S7], thus histological slices produce circular section for each canaliculus.

3. Intraspecific and bilateral variation of dorsal canaliculi

Dorsal canaliculi were present in all segmented anteater (n=8) and long-nosed armadillo (n=6) mandibles (Figure S4). All six long-nosed armadillos displayed an anterior dorsal canaliculi plexus splitting in three to six dorsal foramina (Figure S4*A*-*F*), including the juvenile (Figure S4*F*). A canine, as well as its corresponding dorsal canaliculus, was present in two specimens (Figure S4*A*, *F*). The mandibular canal morphology was similar in the six specimens. The two pygmy anteater (*C. didactylus*, n=2) mandibles presented bilateral variation and showed between 15 and 17 dorsal canaliculi (MNHN 1986-1115, 15L/17R; BMNH 24.12.4.68, 17L/15R; Figure S4*G*, *H*). Bilateral variation was observed in two collared anteaters (*T. tetradactyla*, n=3) and two giant anteaters (*M. tridactyla*, n=3). The collared anteaters (*T. tetradactyla*) showed between 14 (MVZ 153482, 14L/14R) to 17 (ISEM – 788N, 17L/16R) dorsal canaliculi (Figure S4*I*-*K*). The two adult giant anteaters presented 14 (ISEM – 065 V) and 13/14 (MVZ – 185238) dorsal canaliculi, while the juvenile presented slightly more canaliculi with a slightly larger bilateral variation (16L/18R; Figure S4*L*-*N*). Nevertheless, the observed pattern of dorsal canaliculi morphology and distribution along the mandible is similar.

4. Insights into the ancestral number of teeth in anteaters

All known anteater fossil skulls are toothless [S12,S13]. However, our data confirmed that the earliest representatives of the group were toothed, assuming the homology between dorsal canaliculi and alveolar vestiges. There are, however, several limitations in using the number of dorsal canaliculi to estimate tooth number: 1) it is not clear weather bifurcating dorsal canaliculi would correspond to one or more alveoli– although bifurcating dorsal canaliculi mostly appear to correspond to only one tooth in *P. maximus*

595 – which can lead to an overestimation of the number teeth with the present method; 2) a
596 high mandibular canal merges the lower part of the dorsal canaliculi from the posterior
597 part of the mandibular canal of the juvenile *M. tridactyla* makes it difficult to discriminate
598 dorsal canaliculi; 3) intraspecific variation may partly explained the observed number of
599 dorsal canaliculi, especially when comparing the bilateral variation to the interspecific
600 variation observed in other clades within Xenarthra (Cingulata). If we were to reconstruct
601 the dental formula based on the number of dorsal canaliculi regardless of the
602 abovementioned arguments, we would propose that each mandibular quadrant of
603 earliest Vermilinguans comprised between thirteen and seventeen teeth.
604
605
606 **5. Ancestral state estimation of the tree internal nodes**
607 Based on our dataset composed of extant species, we reconstructed the ancestral
608 condition of placental mammals concerning the presence of dorsal canaliculi (Figure
609 S5). We used the re-rooting method of Yang et al. [S14] to perform an ancestral state
610 reconstruction under a continuous time Markov chain. The posterior probabilities for the
611 presence of dorsal canaliculi are presented for each node (Figure S5). We used the
612 same tree as presented in Figure 1, obtained from www.timetree.org [S15]. This tree
613 includes 29 species and 28 internal nodes. Due to the absence of fossil taxa in the
614 analysis, all nodes presented posterior probabilities close to zero or one. The probability
615 of the presence of dorsal canaliculi was high in all nodes within Xenarthra. Excluding this
616 clade, the highest probability for the evolution of dorsal canaliculi was found in the most
617 recent common ancestor (MRCA) of cetaceans (node 12), with 4.86%. We found a
618 0.37% probability for the evolution of dorsal canaliculi in the MRCA of all placentals
619 (node 2). This suggests that the absence of dorsal canaliculi (0) likely corresponds to the

620 ancestral condition of placentals. The ancestral state reconstruction was performed with
621 the phytools package [S16] in R [S17].

Supplemental references

S1. Ulm, C., Kneissel, M., Hahns, M., and Solar, P. (1997). Characteristics of the cancellous bone of edentulous mandibles. Clin. oral Implant. *8*, 125–130.

S2. Kieser, J., Kieser, D., and Hauman, T. (2005). The course and distribution of the inferior alveolar nerve in the edentulous mandible. J. Craniofac. Surg. *16*, 6–9.

S3. Martin, B. (1916). Tooth development in *Dasypus novemcinctus*. J. Morphol. *27*, 647–961.

S4. Ciancio, M.R., Castro, M.C., Galliari, F.C., Carlini, A.A., and Asher, R.J. (2012). Evolutionary implications of dental eruption in *Dasypus* (Xenarthra). J. Mamm. Evol. *19*, 1–8.

S5. Hautier, L., Gomes Rodrigues, H., Billet, G., and Asher, R.J. (2016). The hidden teeth of sloths: evolutionary vestiges and the development of a simplified dentition. Sci. Rep. *6*, 27763.

S6. Anthony, R. (1934). La dentition de l'oryctérope. Morphologie, développement, structure, interprétation. Ann. Sci. Nat. Zool. *17*, 289–322.

S7. Peredo, C., Pyenson, N., Uhen, M., and Marshall, C. (2017). Alveoli, teeth, and tooth loss: understanding the homology of internal mandibular structures in mysticete cetaceans. PLoS One *12*.

S8. Pyenson, N., Goldbogen, J., Vogl, A., and Szathmary, G. (2012). Discovery of a sensory organ that coordinates lunge feeding in rorqual whales. Nature *485*, 498–501.

S9. Greene, E.C. (1955). Anatomy of the rat Second Edi. (New York: Hafner Publishing CO.).

S10. Gray, H. (1995). Anatomy, descriptive and surgical (Bristol: Parragon Book

Service Ltd.).

S11. Thewissen, J.G.M., Hieronymus, T.L., George, J.C., Suydam, R., Stimmelmayr, R., and McBurney, D. (2017). Evolutionary aspects of the development of teeth and baleen in the bowhead whale. J. Anat. *230*, 549–566.

S12. Hirschfeld, S. (1976). A New Fossil Anteater (Edentata, Mammalia) from Colombia, S . A . and Evolution of the Vermilingua. 419–432.

S13. Davit-Béal, T., Tucker, A., and Sire, J. (2009). Loss of teeth and enamel in tetrapods: fossil record, genetic data and morphological adaptations. J. Anat. *214*, 477–501.

S14. Yang, Z., Kumar, S., and Nei, M. (1995). A new method of inference of ancestral nucleotide and amino acid sequences. Genetics *141*, 1641–1650.

S15. Kumar, S., Stecher, G., Suleski, M., and Hedges, S.B. (2017). TimeTree: a resource for timelines, timetrees, and divergence times. Mol. Biol. Evol. *34*, 1812–19.

S16 Revell, L.J. (2012). phytools: an R package for phylogenetic comparative biology (and other things). Methods Ecol. Evol. *3*, 217–223.

S17 Team, R.C. (2013). R: A language and environment for statistical computing.

Table S1. List of all studied specimens with corresponding collection number and voxel size.

Species	Specimen	Voxel size (µm)	Scanning platform
Proteles cristatus	BMNH 34.11.1.5	73.6	BMNH
Canis lupus	LACM 23010	600.0	-
Manis crassicaudata	BMNH 67.4.12.298	59.2	BMNH
Manis javanica	BMNH 9.1.5.858	49.6	BMNH
Orycteropus afer	BMNH 27.2.11.113	116.5	BMNH
Potamogale velox	ZMB 71587	72.0	HZB
Tenrec ecaudatus	Martinez pers. coll.	69.4	RIO
Rhynchocyon petrsi	BMNH 55149	94.0	BMNH
Procavia capensis	UMZC H4980K	86.0	-
Cyclopes didactylus	MNHN 1986-1115	36.0	RIO
Cyclopes didactylus	BMNH 24.12.4.68	32.2	BMNH
Tamandua tetradactyla	BMNH 34.9.2.196	79.8	NMNH
Tamandua tetradactyla	ISEM 788N	57.1	RIO
Tamandua tetradactyla	MVZ 153482	45.1	RIO
Myrmecophaga tridactyla	ISEM 071 N	79.0	RIO
Myrmecophaga tridactyla	ISEM 065 V	74.3	RIO
Myrmecophaga tridactyla	MVZ 185238	63.7	RIO
Bradypus tridactylus	ZMB 18834	41.7	HZB
Bradypus tridactylus	MNHN 1999-1065	113.2	RIO
Choloepus didactylus	ZMB 4949	83.8	HZB

Choloepus hoffmanni	Hautier pers. coll.	83.9	RIO
Dasypus pilosus	ZMB 19240	72	HZB
Dasypus novemcinctus	USNM 033867	36.0	RIO
Dasypus novemcinctus	LSUMZ 8538	36.0	RIO
Dasypus novemcinctus	LSUMZ 29160	36.0	RIO
Dasypus novemcinctus	BMNH 11.10.27.3	58.3	RIO
Dasypus novemcinctus	ZMB 84-357	58.3	HZB
Dasypus novemcinctus	USNM 020920	36.0	RIO
Priodontes maximus	ZMB 47528	72.0	RIO
Tapirus indicus	KUPRI 506	625.0(x,y)x300.0(z)	KUPRI
Molossus molossus	AMNH 234923	20.0	-
Talpa europaea	Martinez pers. coll.	89.0	RIO
Cynocephalus volans	FMNH 56521	65.0	-
Lemur catta	DPC-O92	100.0	-
Tupaia Montana	FMNH 108831	40.0	-
Lepus europaeus	DMET-LE1	137.4	-
Rattus norvegicus	HACB-RN1	54.0	-
Dasyurus hallucatus	TMM M-6921	35(x,y)x78(z)	-

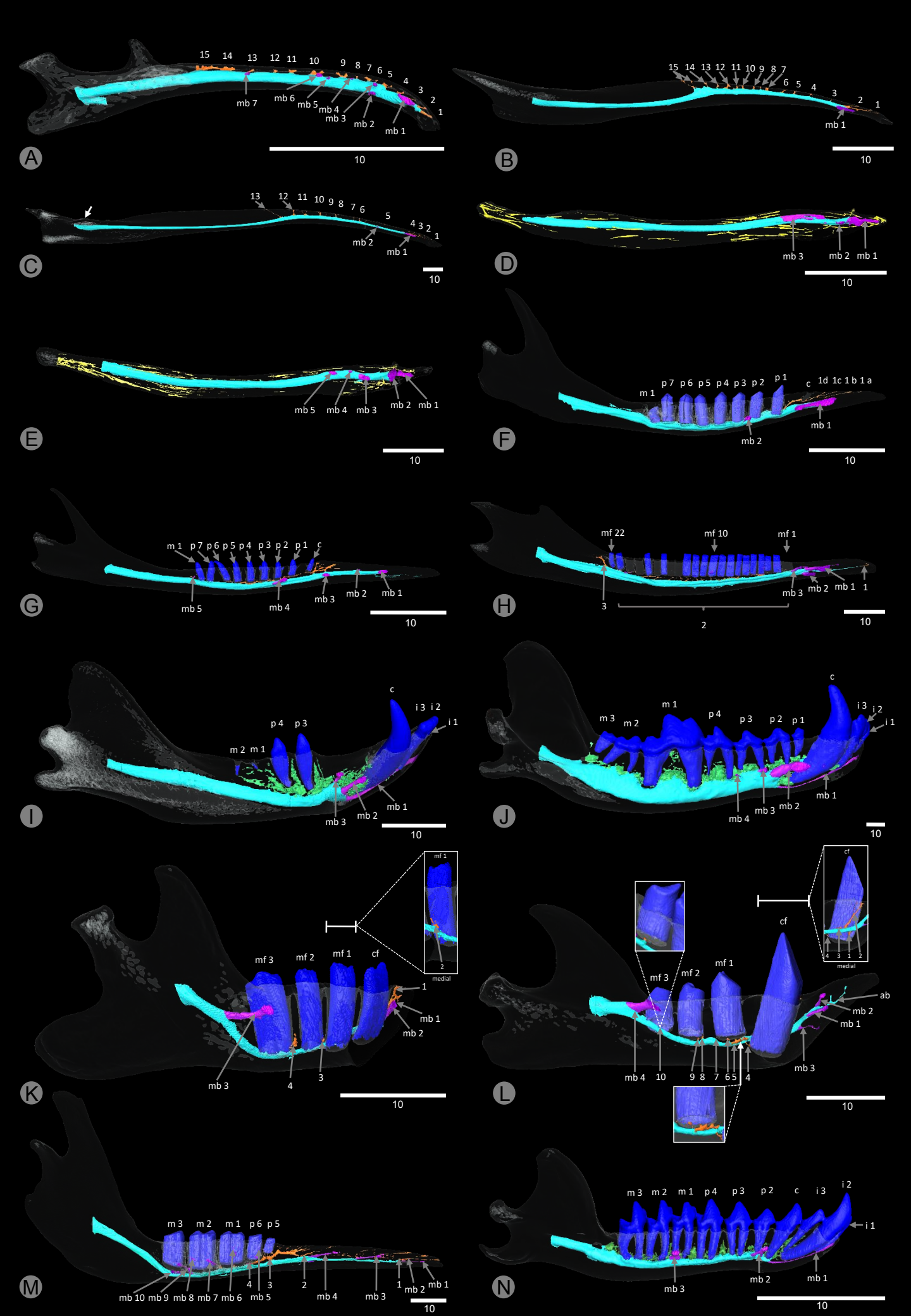
A
15 14 13 12 11 10 9 8 7 6 5 4 3 2 1
mb 7 mb 6 mb 5 mb 4 mb 3 mb 2 mb 1
10
B
15 14 13 12 11 10 9 8 7 6 5 4 3 2 1
mb 1
10
C
13 12 11 10 9 8 7 6 5 4 3 2 1
mb 2 mb 1
10
D
mb 3 mb 2 mb 1
10
E
mb 5 mb 4 mb 3 mb 2 mb 1
10
F
m 1 p 7 p 6 p 5 p 4 p 3 p 2 p 1 c 1d 1c 1b 1a
mb 2 mb 1
10
G
m 1 p 7 p 6 p 5 p 4 p 3 p 2 p 1 c
mb 5 mb 4 mb 3 mb 2 mb 1
10
H
mf 22 mf 10 mf 1
3 2
mb 3 mb 2 mb 1 1
10
I
c i 3 i 2 i 1
p 4 p 3
m 2 m 1
mb 3 mb 2 mb 1
10
J
c
m 3 m 2 m 1 p 4 p 3 p 2 p 1 i 3 i 2 i 1
mb 4 mb 3 mb 2 mb 1
10
K
mf 3 mf 2 mf 1 cf
mf 1
2
medial
1
mb 1 mb 2
mb 3 4 3
10
L
cf
mf 3 mf 2 mf 1
cf
4 3 1 2
medial
ab mb 2 mb 1
mb 4 10 9 8 7 6 5 4 mb 3
10
M
m 3 m 2 m 1 p 6 p 5
mb 10 mb 9 mb 8 mb 7 mb 6 mb 5 4 3 2 mb 4 mb 3 1 mb 2 mb 1
10
N
m 3 m 2 m 1 p 4 p 3 p 2 c i 3 i 2 i 1
mb 3 mb 2 mb 1
10

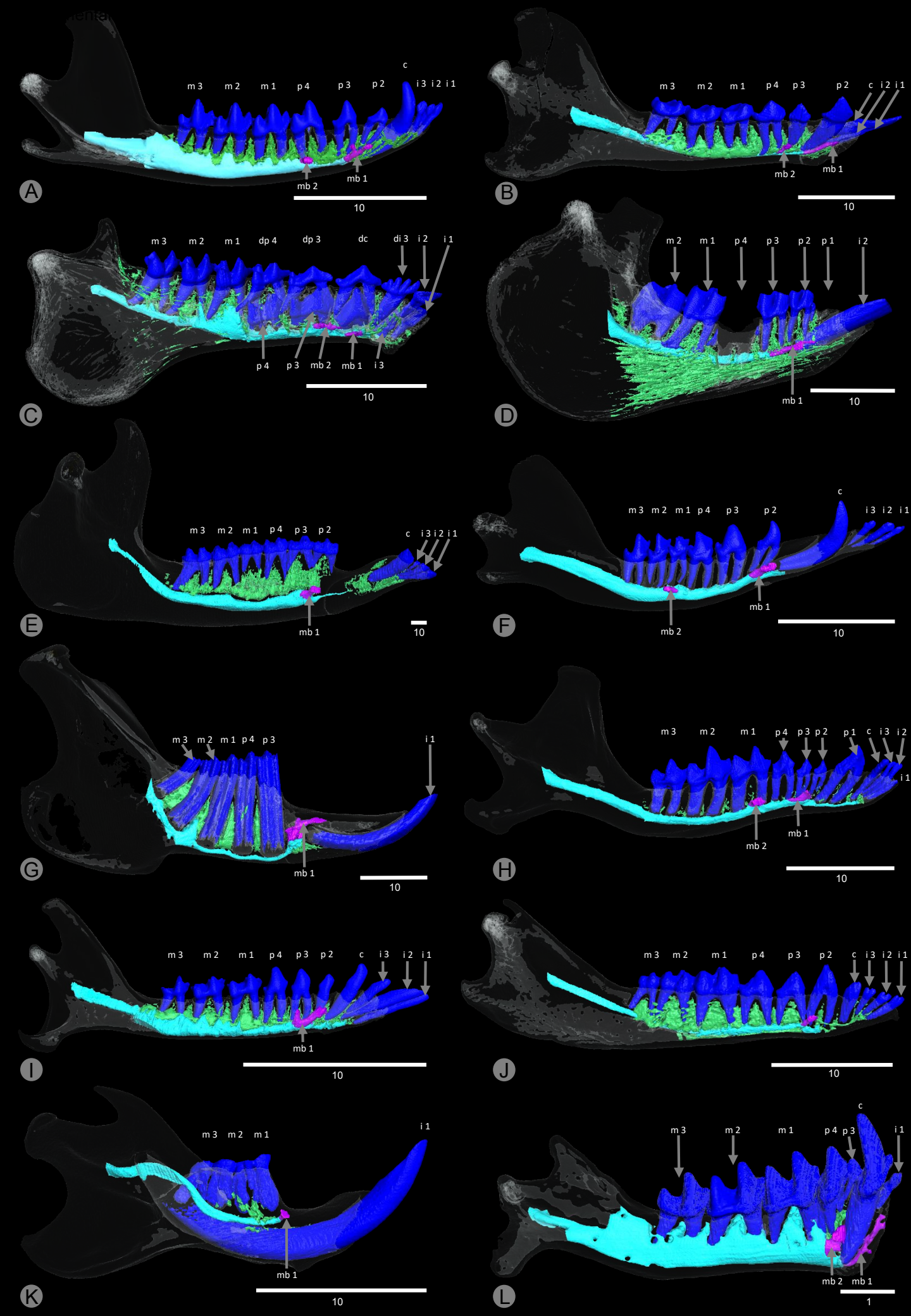
A
m 3 m 2 m 1 p 4 p 3 p 2 c i 3 i 2 i 1
mb 2
mb 1
10
B
m 3 m 2 m 1 p 4 p 3 p 2 c i 2 i 1
mb 2
mb 1
10
C
m 3 m 2 m 1 dp 4 dp 3 dc di 3 i 2 i 1
p 4 p 3 mb 2 mb 1 i 3
10
D
m 2 m 1 p 4 p 3 p 2 p 1 i 2
mb 1
10
E
m 3 m 2 m 1 p 4 p 3 p 2 c i 3 i 2 i 1
mb 1
10
F
m 3 m 2 m 1 p 4 p 3 p 2 c i 3 i 2 i 1
mb 1
mb 2
10
G
m 3 m 2 m 1 p 4 p 3 i 1
mb 1
10
H
m 3 m 2 m 1 p 4 p 3 p 2 p 1 c i 3 i 2 i 1
mb 2
mb 1
10
I
m 3 m 2 m 1 p 4 p 3 p 2 c i 3 i 2 i 1
mb 1
10
J
m 3 m 2 m 1 p 4 p 3 p 2 c i 3 i 2 i 1
10
K
m 3 m 2 m 1 i 1
mb 1
10
L
m 3 m 2 m 1 p 4 p 3 c i 1
mb 2
mb 1
1

Supplemental Figure S3

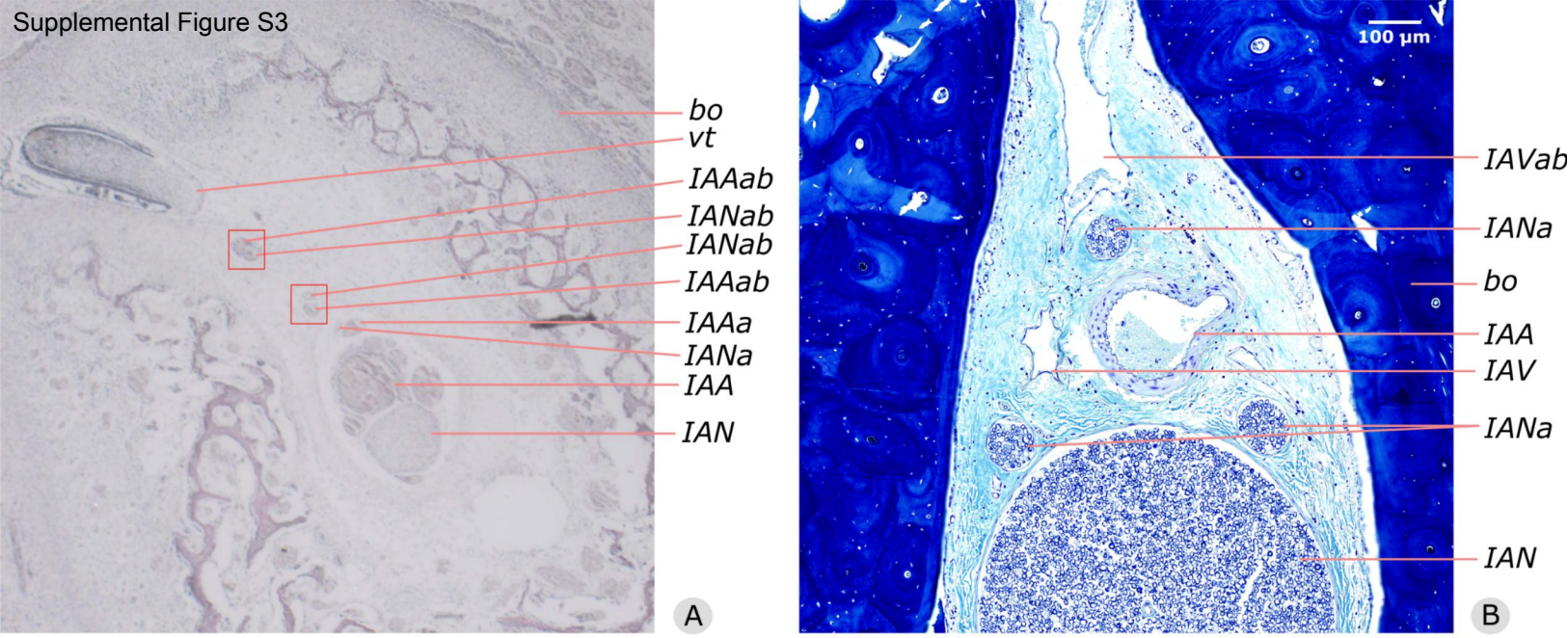

Supplemental Figure S4

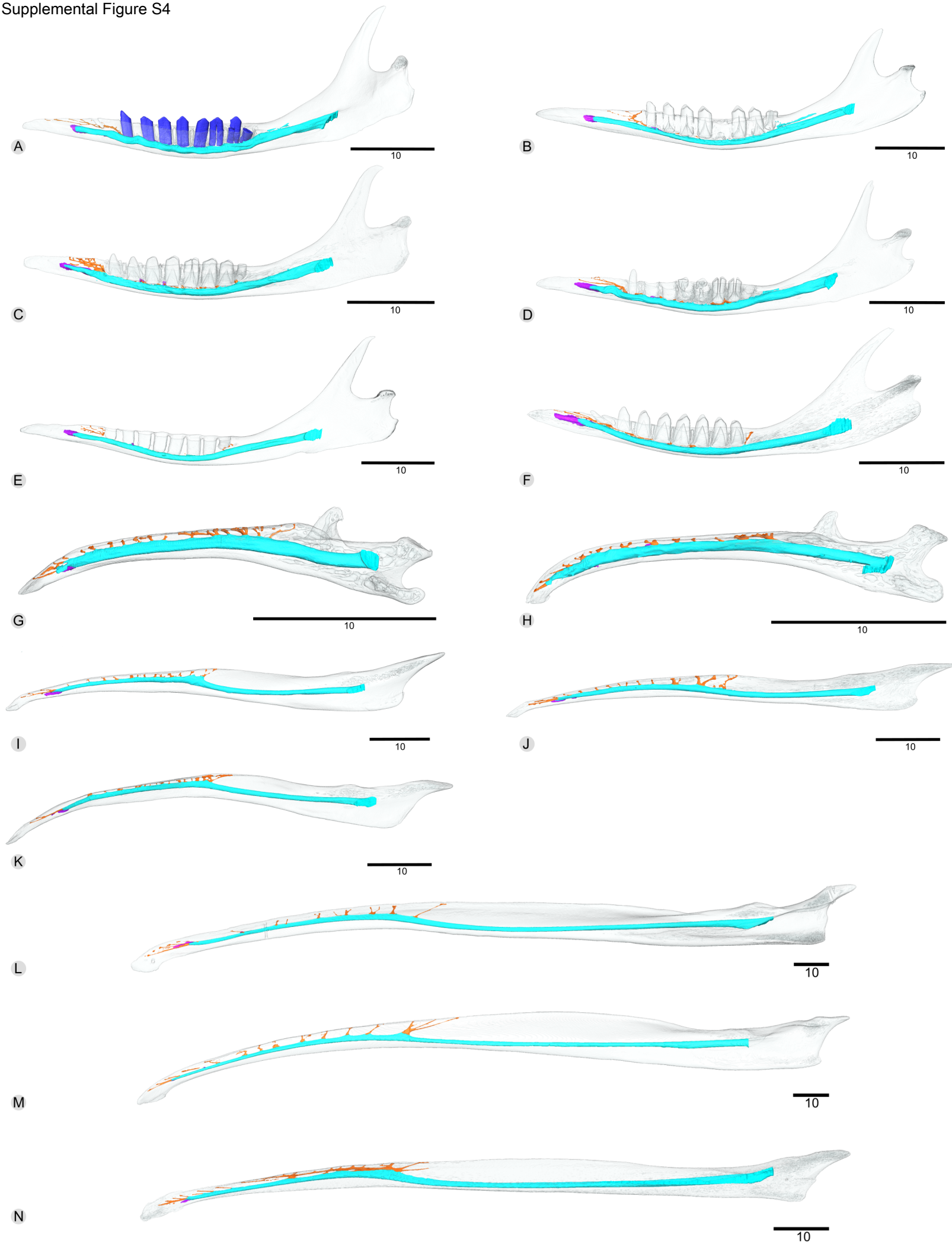

Supplemental Figure S5